TRENDS IN SEASONAL CLIMATE VARIANCE IN THE SUBTROPICAL RESERVOIR JOE POOL LAKE, TEXAS: IMPLICATIONS DISSOLVED OXYGEN AND NUTRIENT DISTRIBUTION

by

REBEKAH BALL

Presented to the Faculty of the Graduate School of

The University of Texas at Arlington in Partial Fulfillment

of the Requirements

for the Degree of

MASTER OF SCIENCE IN ENVIRONMENTAL SCIENCE AND EARTH SCIENCE

THE UNIVERSITY OF TEXAS AT ARLINGTON

May 2015

Acknowledgements

This work was supported by the Department of Earth and Environmental Science, Climate Group, supervised by Dr. Arne Winguth, the Department of Biology Limnology Lab, ,Dr. Jim Grover, and Master of Science committee member Dr. Elizabeth Griffith, with assistance from Garret Haynes, Angela Osen, Taylor Hughlett, Brandi Kelp, Jay Jones, and Nguyen Cao. Graphs of time series were done on computers of the National Center for Atmospheric Research, which is funded by the National Science Foundation (NSF). The access of computer resources was supported by NSF Grant EAR-0745817.

March 20, 2015

Abstract

TRENDS IN SEASONAL CLIMATE VARIANCE IN THE SUBTROPICAL RESERVOIR JOE POOL LAKE, TEXAS: IMPLICATIONS OF DISSOLVED OXYGEN AND NUTRIENT DISTRIBUTION

Rebekah Ball, MS

The University of Texas at Arlington, 2015

Supervising Professor: Arne Winguth

The primary causes of seasonal variance in temperature, hydrological cycle, and nutrient distribution of lakes, and the processes explaining these changes including climate change and land use changes have been investigated for several decades because the importance of lakes for water resources, recreation, and sensitive ecosystems. Many of the previous studies, however, have been focused predominately on natural lakes in temperate climates and not on subtropical reservoirs.

In this study a seasonal survey of temperature, turbidity, dissolved oxygen, and nutrients on the Joe Pool reservoir in North Central Texas has been conducted almost weekly from November 21st of 2012 through November 20th of 2013 and compared with meteorological data from the National Weather Service and Western Regional Climate Center and with previous seasonal lake measurements. Measured lake temperatures during sampling ranged from 6.5 °C in winter to 30.0°C in summer. Lake mixing was enhanced during spring and fall with wind speeds exceeding 5 m s^{-1} due to frontal systems and thunderstorms leading to uniform vertical oxygen and nutrient distribution. During May to June, increased solar radiation leads to increases in air and lake surface temperatures, thus increasing the vertical thermal gradient and stratification in the lake.

Dissolved oxygen declines during these months and soluble reactive phosphorus increases in response to these physical changes.

The amplitude of the seasonal cycle decreased compared to surveys from 1991 through 1992 and from 1999 through 2001, potentially attributed to long-term fluctuations in climate that are likely attributed to climate variability, such as Mt. Pinatubo eruption and ENSO, and long-term climate change. Since the impoundment of water into Joe Pool Lake in 1986, nutrient concentrations decreased through time potentially due to reservoir aging.

Table of Contents

List of Illustrations

List of Tables

Chapter 1

Introduction

Historical investigation of lake and reservoir systems has focused primarily on north temperate lakes, but in recent years the importance of both the similarities and differences amongst lake and reservoir systems in different climate zones have been investigated. Various factors influence the physical and biogeochemical states of lakes and reservoirs such as extreme weather events, climate variability and climate change, eutrophication, acidification, land use changes and other anthropogenic impacts (Cottingham 1998; Jeppesen et al. 2005; Mulholland 1997). Reservoirs are affected by reservoir aging, an accumulation of organic and inorganic matter in sediments by various processes, which leads to a reduced basin volume and nutrient residence time (Purcel and Weston 1939; Walker et al. 2007; Thorton et al. 1996). Unlike natural lakes, reservoirs generally are characterized by sectionality, with one section near the dam that displays lacustrine characteristics; one section near the inflow that displays riverine characteristics; and a transitional section between the two (Walker et al. 2007).

Changes in weather and climate patterns will change the temporal patterns of parameters such as temperature, precipitation, soil moisture, lake level, and albedo (Magnuson et al. 1997; Lewis 1973; Taranu 2010). Reservoir ecosystems are subject to shifts among multiple locally stable states (Holling 1973) that may be controlled by seasonal fluctuations in nutrient concentrations caused by reservoir temperature and irradiance. Climate change is likely to cause prolonged, and intense periods of vertical thermal stratification (Holling 1973) which could favor hypoxic to anoxic conditions by an increased vertical gradient in the biological pump (De Stasio et al. 1996). Other implications of the effects of climate change on aquatic systems consists of decreased

duration of seasonal lake ice, nutrient loading and residence time, and changes in lake morphometry (Blenckner 2005; Taranu et al. 2010).

Lakes and reservoirs have has been intensively investigated in the Northern U.S. states and in Canada, but to lower extent explored in Southern U.S. reservoirs (Grover and Chrzanowski 2000; Magnuson et al. 1997; Marshall and Peters 1989; Schindler 1971; Yannarell et al. 2003). Lakes and reservoirs are typically classified by trophic levels (Naumann 1919) or by mixing (Hasler 1947; Mortimer 1952), e.g. following the classification from Hutchinson and Löffler (1956) and Hutchinson (1957). A more comprehensive revision of these classifications was created by Lewis (1983) and will be used in this study (Table 1.1). The annual mixing and stratification

Table 1.1 Lewis mixing classification (Lewis 1983).

Classification	Description
amictic	always ice-covered
cold monomictic	ice-covered most of the year, ice-free during the warm season, but not warming above 4°C
continuous cold polymictic	ice-covered part of the year, ice-free above 4°C during the warm season, and stratified at most on a daily basis during the warm season
discontinuous cold polymictic	ice-covered part of the year, ice-free above 4°C and stratified during the warm season for periods of several days to weeks, but with irregular interruption by mixing
dimictic	ice-covered part of the year and stably stratified part of the year with mixing at the transitions between these two states
warm monomictic	no seasonal ice cover, stably stratified part of the year, and mixing once each year
discontinuous warm polymictic	no seasonal ice cover, stratifying for days or weeks at a time, but mixing more than once per year
continuous warm polymictic	no seasonal ice cover, stratifying at most for a few hours at a time

events used for these classifications are created by changes in the stability of the water column owing to fluctuations in water density from seasonal temperature changes or mechanical mixing by wind and wave action.

The seasonality of temperature-induced mixing and stratification effects the distribution of dissolved oxygen and nutrient concentration. Seasonal mixing trends are well established; however temporal variance within a reservoir may occur due seasonal variability as well as reservoir aging. Overturning of lake's water masses generally occurs during the period from fall to spring as cooler water masses overturn (De Stasio 1996; Lampert and Sommer 2007). In subtropical regions vertical mixing under ice-free conditions with cold air outbreaks during winter lead to rapid surface cooling, reduction in the vertical temperature gradient producing density instabilities, thus results in vertical uniform distribution of dissolved oxygen and nutrient concentration (Monson 1992; Sterner 1994). During winter, when lowest lake temperatures are observed, dissolved oxygen concentration is maximal because solubility of oxygen in water is inversely proportional to the temperature (Weiss 1970; Lampert and Sommer 2007; Monson 1992). During summer, stratification by a pronounced thermocline (Boehrer and Schultze 2008) leads to depletion of dissolved oxygen below the thermocline primarily because the decay of organic material as well as by respiration of organisms exceeds the supply of oxygen by mixing from the surface. Under these conditions, anoxic conditions (Stefan 1989) can occur particular during a period of calm conditions with maximal vertical stratification and high flux of particular organic carbon into the deeper lake. Stratification also causes low concentrations of nutrients in the epilimnion and higher concentrations in the hyplolimnion because organisms consume the nutrients within the epilimnion (Boehrer and Schultze 2008). Low fall to winter surface temperatures and thus low vertical temperature gradients, the occurrence of high wind speeds, and high rates of

precipitation are expected to create a well-mixed lake environment with higher concentrations of nutrient distributed throughout the water column. High spring and higher summer water temperatures, increased UV radiation, and calm conditions are expected to promote stable stratified conditions with lower overall nutrient concentrations due to nutrient depletion by algae in the euphotic zone.

Net primary production in a reservoir is typically influenced by temperature, light, macro and micro nutrient availability and mixing (Walker et al. 2007). Reservoir stratification affects the vertical nutrient gradient (Sterner 1994) because enhanced vertical stratification leads to depleted nutrient concentration in the surface and thus reduced vertical organic matter flux from the euphotic zone into the deeper reservoir. The vertical distribution of nutrients is primarily controlled by the mixing regime and biotic activity (Celik and Schindler 2006). When stratification occurs, nutrients in the upper layers become depleted due to the uptake of nutrients by phytoplankton, and because vertical mixing of nutrient-rich bottom waters is suppressed under these conditions (Celik and Schindler 2006). Nutrient depletion can also occur, if nutrient inventory declines, which can be influenced by the reservoir age. Reservoirs generally are found to have a much larger nutrient inventory immediately after its impoundment due to the decomposition of submerged terrestrial vegetation (Purcel and Weston 1939). Over time the former terrestrial vegetation will be depleted and the nutrient inventory will adjust to near-steady state condition (Purcel and Weston 1939). Riverine nutrient input by precipitation linked to frontal systems and thunderstorms, influenced by the position of the subtropical jet stream, wind-blown transport of dust or increase in evapotranspiration and lateral differences within the reservoir also affect the nutrient concentration and distribution (Carey 2013; Chrzanowski and Grover 2005; Paulson et al. 1991). Horizontal gradients in nutrient distribution due to runoff in shallow areas with increased

photosynthesis occur in both lakes and reservoirs (Walker et al. 2007). Reservoirs, however, tend to have greater nutrient gradients than natural lakes due to the inflow of water from tributaries and the slowing of this water by a dam (Walker et al. 2007). Such a nutrient gradient, from inflow to dam, found in many reservoirs is generally divided into three sections: riverine, transitional, and lacustrine, based on what processes dominate the section (Kennedy and Walker 1990; Kimmel and Groeger 1984; Kimmel et al. 1990; Søballe et al. 1992). Since net primary productivity is dependent on temperature increased research of the effects climate change on ecosystem have been investigated in recent years (Grover and Chrzanowski 2005; Meerhoff et al. 2007; Mulholland et al. 1997; Reynolds 1984; Sommer et al. 1986).

Excessive nutrient loading of lakes and reservoir stimulates eutrophication, photosynthesis and organic matter production thus decreasing the water clarity (Table 1.2) and increasing toxic algae population (Jeppesen et al. 2005; Mackenzie et al. 2001). These environmental changes cause severe ecological problems for example decline in the food web complexity and biodiversity. An aquatic system is classified as eutrophic based on average total nitrogen concentration (TN), total phosphorus concentration (TP), chlorophyll a concentration (Chl a), and Secchi disk depth (Table 1.2). The severity of the effects of increased nutrient loading on reservoir ecosystems is dependent on lake primary production, water depth, and climate (Lampert and Sommer 2007; Walker et al. 2007).

Acidification by decreasing pH levels of reservoirs can be triggered from natural and anthropogenic sources. Deposition of atmospheric carbonic acid, formation of organic acids owing to organic detritus, and leaching of hydrogen ions from bedrock are the primary natural sources of acidity (Gorham et al. 1986). The primary anthropogenic sources are sulfuric acid formed in the atmosphere from the oxidation of sulfur dioxide

emissions, from coal fired power plants as well as industrial processes, and nitric acid formed from nitrogen input from fertilizers and fossil fuel combustion (Vitousek et al. 1997). Acidification eliminates most macrophytes and many other organisms native to lake ecosystems. The native species are replaced with species that are resistant to lower pH and diversity generally decreases. Another concern of lake acidification is the increased invasion of anthropogenic CO_2 by global fossil fuel combustion and land use changes into aquatic bodies, because the atmospheric CO2 concentration rose from about 280 ppmv in 1850 to 398 ppmv in 2014 (Gorham et al. 1986; Feely et al. 2009;http://www.esrl.noaa.gov/gmd/ccgg/ trends/global.html).

Table 1.2 Classification of trophic states in lakes adapted from Nurnberg (1996).

Trophic state	TP (µmol L^{-1})	TN (µmol L^{-1})	Chl *a* (mg $L^{-1)}$	Secchi depth (m)
Oligotrophic	<25	<0.32	<0.0035	>4
Mesotrophic	25-46.4	0.32-0.97	0.0035-0.009	4-2
Eutrophic	46.4-85.7	0.97-3.23	0.009-0.025	2-1
Hypertrophic	>85.7	>3.23	>0.025	<1

Chapter 2

Objectives

2.1 Introduction

The site investigated in this study is one of the most well investigated subtropical reservoirs is Joe Pool Lake in North Texas with shorelines in Tarrant, Dallas, and Ellis counties. Construction of Joe Pool Lake began in 1977 and the lake was impounded in January 1986 and is located at 32.64458 °N and -96.99306 °W on the Eagle Ford Formation (Figure 2.1). Joe Pool Lake is part of the Trinity River Basin and receives river runoff from the Mountain Creek and Walnut Creek. The reservoir has a maximum depth of 23 m and drains an area of 601 km^2 (Figure 2.1) and a storage capacity of 0.2182 km^3 and is 31.3 km^2 (www.swf-wc.usace.army.mil/ joepool/). Hydrographic and biological surveys Joe Pool Lakes have been performed for several decades including a comprehensive investigation for the period 1991 to 1992 (Sterner 1994) and 1998 to 1999 (Grover and Chrzanowski 2004).

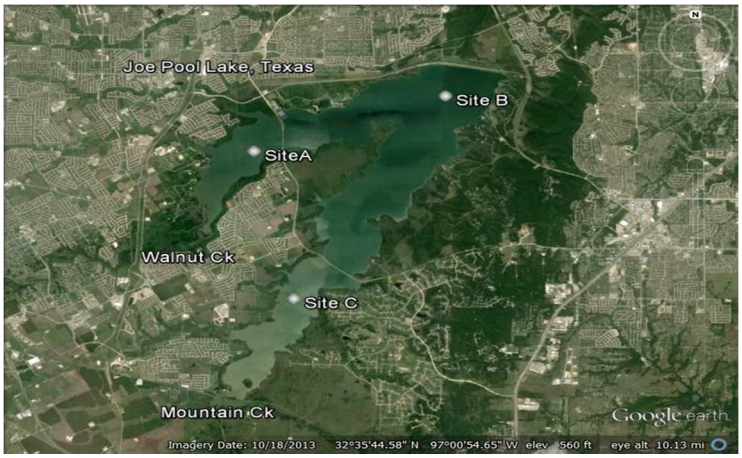

Figure 2.1 Map of Joe Pool Lake with the approximate locations of sites A (N 32.61973 and W 97.04616), B (N 32.63599 and W 96.99614), and C (N 32.57603 and W 97.03451).

Joe Pool Lake has classified as warm monomictic (Sterner 1994) according to the Lewis revised classification (Table 1.1; Lewis 1983) while Grover and Chrzanowski (2004) determined the trophic state of Joe Pool Lake to be mesotrophic based on nutrient concentrations and chlorophyll populations. The lake's persistent high turbidity is highly linked to transport of fine-grained calcareous clay particles from the adjacent land and resuspension of limestone sedimentary deposits. Thus, the Secchi disk depth in Joe Pool Lake cannot be used to determine its trophic state (Figure 2.2), because the Secchi disk depth is inversely related to the turbidity, which depends on both the biogenous and terrigenous particles concentration.

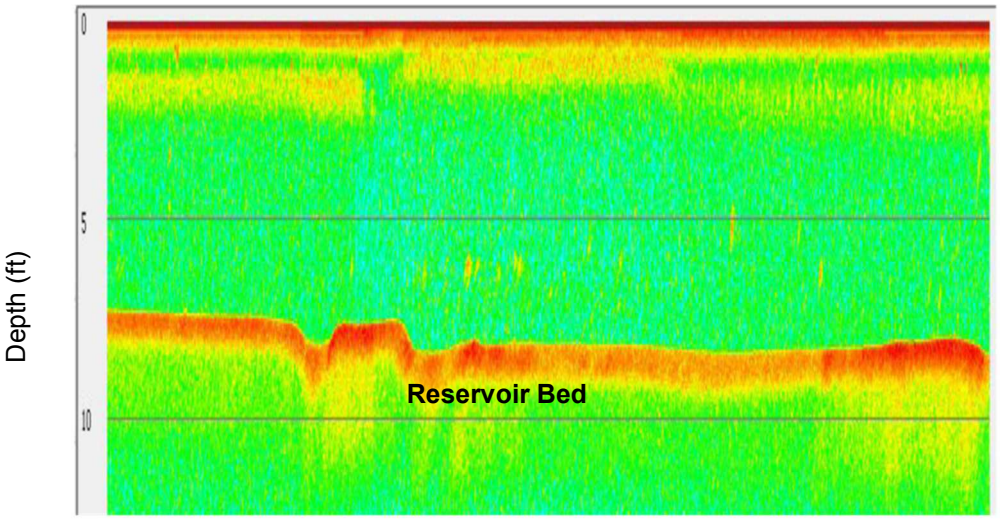

Figure 2.2 Sonar image showing high turbidity within Joe Pool Lake. Location of image near site C (N 32.7210 and W 97.4417).

This study focused on a seasonal hydrographic survey of the North Texas reservoir Joe Pool Lake including measurements of air and lake temperature, wind speed, Secchi disk depth, dissolved oxygen and nutrient concentration throughout the water column at three distinct sites documented in Sterner (1994); one at each of the two

inlets from Mountain Creek and Walnut Creek and another near the reservoir dam (Figure 2.1). Lake temperature data were used to determine how lake's stratification in conjecture with Secchi disk data affect distribution of dissolved oxygen and macro-nutrients. During winter, cool surface temperatures and high wind speeds are expected to create a well-mixed lake environment with uniform vertical nutrient gradients throughout the water column. During summer an increase in incoming solar radiation enhances vertical stratification within the lake and nutrient-depleted surface water by primary production in the euphotic zone, and thus vertical gradients in nutrient concentration. Nutrient input from Mountain and Walnut Creeks by thunderstorms are likely to occasionally contribute to elevated nutrient concentrations and hence primary production.

The goal of this study is to collect and analyze a time series of temperature, precipitation, dissolved oxygen and nutrients at Joe Pool Lake and compare it with previous surveys (Chrzanowski and Grover 2005; Grover and Chrzanowski 2004; Sterner 1994) to better understand the seasonal climate variability and climate changes in the physical and biogeochemical conditions of a subtropical reservoir while the reservoir became siltated and urbanized over time.

Climate variability like drought linked to El Niño Southern Oscillation; a two to seven year cycle in sea surface temperature(SST) that produces climactic variation in the tropics and subtropics; (ENSO; Bjerkness 1969) can lead to remarkable differences in hydrographic properties. For example during the 2011-2012 Texas drought a record heatwave led to enhanced thermal stratification and surface nutrient depletion whereas more well-mixed conditions occur during non-drought years (Nieslen-Gammon 2012). During an El Niño year, warmer SST, increased convection, and strong westerlies in the central and eastern North Pacific produce a strong subtropical Jetstream, while during an La Niña year the opposite occurs (Bjerkness 1969). In North Texas, the El Niño phase

causes higher precipitation which can lead to enhanced riverine nutrient input whereas warmer surface temperatures lead to enhanced vertical temperature and nutrient gradients in Joe Pool Lake (Bjerkness 1969; Walker et al. 2007). The Atlantic multidecadal oscillation (AMO), a decadal sea surface temperature fluctuation in the North Atlantic and North Atlantic oscillation (NAO), a pressure anomaly between the Iceland low pressure system and the Bermuda high pressure system, influence air temperatures and precipitation rates in the North Atlantic region (Bjerkness 1964; D'Aleo and Easterbrook 2010). For example, the AMO cooling phases producing cooler air temperatures and increased precipitation and the warming phase producing the opposite effect while NAO negative phases producing cooler air temperatures and decreased precipitation and the positive phase having the opposite effect (D'Aleo and Easterbrook 2010). Changes in wind speed due to a shift in 2000 from a positive phase to a negative phase of the Interdecadal Pacific Oscillation (IPO); which is decadal climate variability of sea surface temperature and mean sea level pressure; may also effect the vertical stratification at Joe Pool Lake (England et al.2014; Salinger et al. 2001).. Volcanic eruptions, like that of the Mount Pinatubo in 1991 before the survey of Sterner (1994), was thought to lead to a cold bias and enhanced vertical mixing from 1991 through 1996. Urban development and associated fertilizationion of rivers likely amplifies nutrient input into Joe Pool Lake thus enhancing the productivity and organic matter formation. The particle concentration is also amplified by increased particle input from runoff near urbanized areas.

2.2 Does seasonality of temperature, oxygen, and nutrient concentration in Joe Pool Lake change over time?

The effects of seasonality on temperature, oxygen, and macro nutrients in a subtropical reservoir, Joe Pool Lake, is the primary focus of this study. The effects of seasonal air temperature, wind speed, and precipitation on thermal stability within Joe Pool Lake were explored. The influence of seasonal lake temperature on oxygen and macro nutrient distribution has also been analyzed.

Variations in Joe Pool Lake stratification and nutrient distribution are influenced by vertical temperature gradients, wind speed, UV radiation, and precipitation. Low surface temperatures during the winter season lead to enhanced mixing and low vertical temperature gradients. In addition, high frequency of elevated wind speeds contribute to a well-mixed lake environment and increased surface nutrient concentration. In Joe Pool Lake during spring and fall, concentrations of riverine nutrient-input by intense precipitation contribute to elevated nutrient concentration. In the summer season, increased shortwave radiation leads to vertical stratification and to enhanced export of organic matter from the euphotic zone into deeper layers leads to nutrient depletion.

2.3 If seasonality change over time, which dominant climatic process control long-term change in seasonality of lake mixing, turbidity, oxygenation, and nutrients in Joe Pool Lake?

Changes in nutrient cycling and turbidity were analyzed to gain understanding of the effect of reservoir aging on a subtropical reservoir by using data from this study compared with Sterner (1994) and Grover and Chrzanowski (2004). Secchi disk depth, nutrient, and oxygen distribution were analyzed to determine whether changes in trophic state and possibly lake mixing occurred due to the aging of the reservoir. The effects of

variations in ENSO, thought to be the major control over long term change, and the Mt. Pinatubo eruption in 1991 was also explored.

Reservoir aging will likely cause a decrease in nutrient concentrations and increase in siltation. These long-term climatic anomalies can change the mixing regime of the lake and mixing classification (Lewis 1983). Eventually nutrient concentrations may increase with increase in reservoir age causing a shift from mesotrophic to eutrophic conditions (Table 1.2). Environmental data is likely to depict long term changes in the environmental conditions within the study area. Increased monthly air temperatures accompanied by lower precipitation are likely, particular during the 2011-2014 Texas drought linked to a strong La-Niña phase (Nieslen-Gammon 2012). Wind speeds may also have increased due to the Interdecadal Pacific Oscillation (IPO) shifting from a positive phase to a negative phase in 2000 (England et al. 2014).

Chapter 3

Methods

3.1 Introduction

Three sites were selected, within the Joe Pool Lake, to study temporal variations in water temperature, nutrient, and oxygen distribution. Site visits to all three were conducted almost weekly for one year beginning in November 21, 2012 and ending in November 20, 2013. Measurements were not conducted when wind speed exceeded 10 m s^{-1}, or lightning or mechanical failure of the boat occurred (a total of seventeen surveys of which six were due to mechanical failure of the outboard engine). The three site locations were chosen based on the locations of Sterner (1994): site B near the reservoir dam and sites A and C in each of the creeks (lake arms) feeding into the reservoir (Figure 1.1). Site A is located in the arm of the lake fed by Walnut Creek, and site B is in the arm fed by Mountain Creek.

3.2 Instruments used in the Lake Study

At each weekly survey, meteorological observations including, wind speed, wind direction, and air temperature, humidity, and dew point were measured with an Extech 45158 mini thermo-anemometer plus humidity meter. Cloud cover were estimated on octa scale from zero to eight with zero being clear sky and eight being overcast.

In the lake, vertical profiles of temperature, dissolved oxygen, and salinity were measured at one-meter intervals by at least two of the available instruments: a YSI30, YSI55, and YSI2030. In these instruments, temperature is measured by a thermistors sensor. The YSI55 and YSI2030 measure the dissolved oxygen concentration with polarographic sensors and YSI30 and YSI2030 include a conductivity sensor. Salinity is estimated from the conductivity using the (UNESCO 1981). Spatial and temporal

gradients were insignificant relative to the mean values for this region. All instruments were calibrated and instrument error were recorded in Table 3.1 using the methods specified by the operator's manuals.Measurements during high wind speeds and waves could lead to

Table 3.1 Instrument used in this study and their accuracy. Note that instrument errors specified by manuals listed below may differ in the Lake study.

Instrument	Instrument Accurarcy
YSI 55 Dissolved Oxygen sensor	±0.3 mg/L
YSI 55 Temperature sensor	±0.2 °C
YSI 30 Temperature sensor	±1.50%
YSI 30 Salinity sensor	±2.0%
YSI 2030 Dissolved Oxygen sensor	2% of the reading or ±0.2mg/L, whichever is greater
YSI 2030 Temperature Senser	±0.3 °C
YSI 2030 Salinity sensor	±0.1
Extech 45158 Wind Speed	3% or ±0.11 m/s
Extech 45158 Temperature	±1.0 °C
Extech 45158 Relative Humidity	5% RH
Extech 45158 Dew Point	±2.0 °C
Secchi disk (Talley)	± 0.1

significant errors causing the sensor oscillated around the vertical axis thus causing inaccuracy in the estimate of the depth. Water depth was measured by a meter-marked rope with a lead weight and by Humming Bird Sonar 497 ci HD (depth capability 365 m, sonar operating frequencies 83 kHz , and 200 kHz , scan area 60° at 10 dB in 83 kHz,

and 20° at 10 dB in 200 kHz). Water samples were taken using a Van Dorn sampler lowered to various depths and placed in a cooler with ice while being transported from the field to the lab. Samples were taken at each of the sample sites two samples were taken at the 0.5 meter depth, one to be filtered and the other kept unfiltered both sets. Once in the lab, the samples were kept frozen and in the dark until the time of analysis. Sets of two samples were then taken at various depths dependent upon the thermocline present at the individual sites, taking at least four samples with two above the thermocline and two below. Secchi disk depth was measured with a Secchi disk with a diameter of 0.20 meter by lowering the disk vertically into the water until it is no longer visible. The depth the disk is beneath the water is then recorded as the Secchi depth. The Secchi depth is inversely related to the attenuation which is influenced by the amount of suspended particles in the water, both organic and inorganic, in the path of sight (Preisendorfer 1986).

3.3 Chemical Nutrient Analysis

Of the pairs of water samples collected, half were filtered in the laboratory using 0.2 µm 47mm glass fiber filters and the other half kept unfiltered. All samples were frozen until time of analysis. The soluble reactive phosphorus (SRP) analysis uses filtered samples treated with a phospho-molybdate complex to reduce the phosphorus, allowing the absorbance to be measured using a Hitachi spectrophotometer (Strickland and Parsons 1972; with modifications developed in lab by U. Sommer; Appendix A).

The total phosphorus (TP) analysis used unfiltered samples that undergo oxidation due to the addition of a persulfate oxidation reagent and sixty minutes in an autoclave. After oxidation, the samples are filtered using 0.45 µm cellulose filters; pH is

corrected to approximately 8.3, and then treated as in the soluble reactive phosphorus analysis (Menzel and Corwin 1965; Strickland and Parsons 1972; Appendix B).

Nitrite content is measured using a sulfanilamide solution to create a diazo compound that reacts with a naphthylethylene solution to form a highly colored azo dye that is then measured using a Hitachi spectrophotometer (Strickland and Parsons 1972; Wetzel and Likens 1991; Modifications developed by T.H. Chrzanowski 2000; Appendix C). On the same day, the corresponding nitrate samples were analyzed by using spongy cadmium shaken with a small volume of sample and buffered using Strickland buffer reduces nitrate to nitrite which is then analyzed using the methods mentioned above for nitrite analysis (Jones 1984; Strickland and Parsons 1972; Wetzel and Likens 1991; modification developed by T.H. Chrzanowski (2000) and Grover (2013); Appendix D).

The ammonium analysis uses a phenol solution, an oxidizing solution, and a catalyzing nitroferricyanide solution, which together forms a blue indophenol with ammonia that is measured using a Hitachi spectrophotometer (Solorzano et al. 1969; Strickland and Parsons 1972; Appendix E).

For the soluble reactive silicate analysis, samples are allowed to react with molybdate under conditions which result in the formation of silicomolybdate, phosphomolybdate, and arsenomolybdate complexes. A reducing solution, containing metol and oxalic acid, is then added which reduces the silicomolybdate complex to give a blue reduction compound and simultaneously decomposes any phosphomolybdate or arsenomolybdate, so that interference from phosphate and arsenate is eliminated (Strickland and Parsons 1972; Appendix F).

Chapter 4

Results

4.1 Seasonal Variation of Joe Pool Lake's Physical and Geochemical Properties

In this study, water mass characteristics and mixing identified from previous work (Sterner 1994; Chrzanowski and Grover 2005; Grover and Chrzanowski 2004) have be re-examined by new measurements taken in 2012 and 2013 (section 2) in order to identify any temporal seasonal changes in the lake's stratification.

During winter (December- February) average surface air temperatures ranged from 8.8 °C to 14.4 °C and moderate winds with a maximum of 3.8 m s-1 (Figure 4.1; Figure 4.2). Daily precipitation from NOAA, was low with a small peak of 8.9 cm in January (Figure 4.3; http://www.ncdc.noaa.gov/cdo-web/datasets/GHCND/stations/GHCND:USC00414597/detail). During this time the

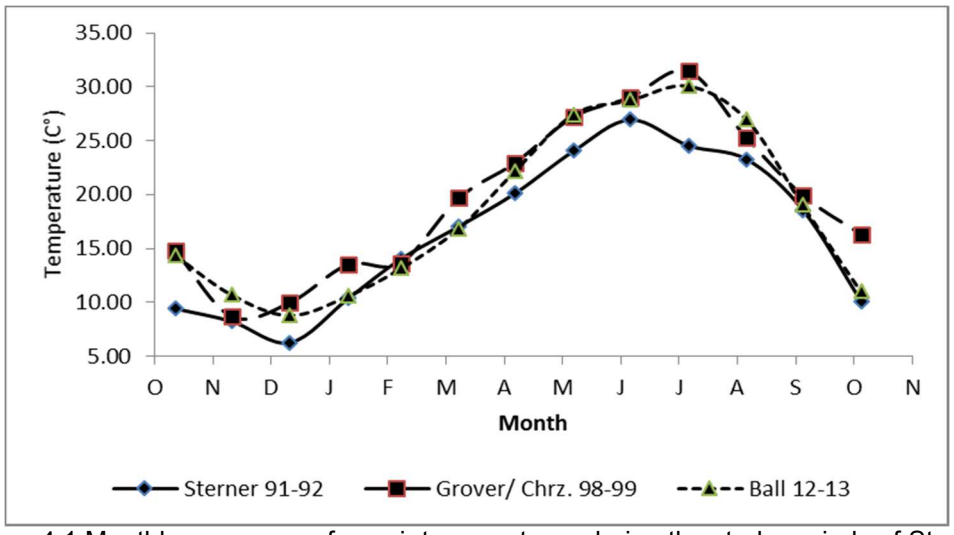

Figure 4.1 Monthly average surface air temperatures during the study periods of Sterner (1994), Grover and Chrzanowski (2005), and the present study. Data were compiled from the National Oceanic and Atmospheric Administration and the Western Regional Climate Center.

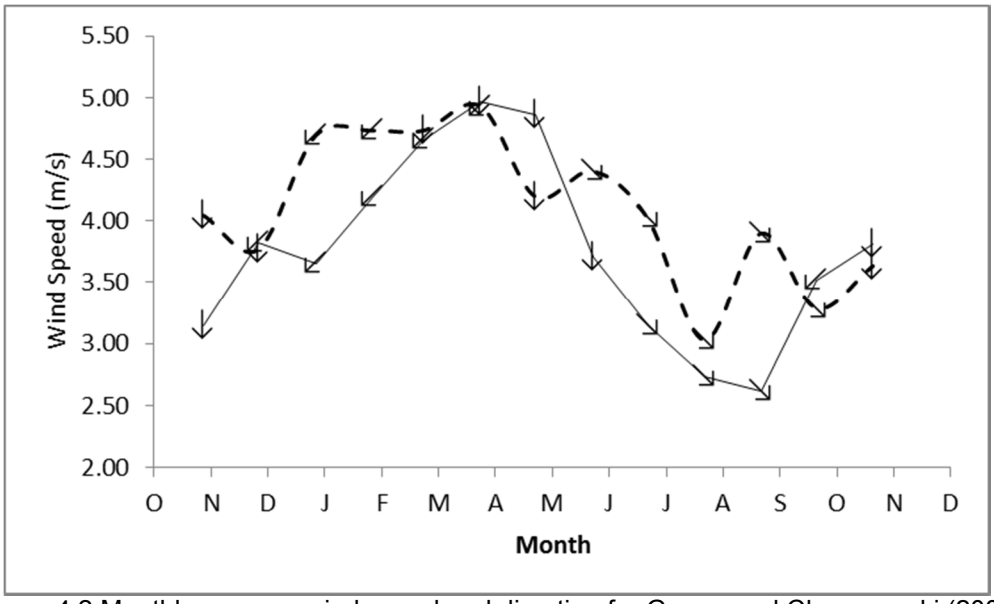

Figure 4.2 Monthly average wind speed and direction for Grover and Chrzanowski (2005; dashed line) and the present study (solid line). Data are compiled from the National Oceanic and Atmospheric Administration Dallas Love Field Airport station 13960.

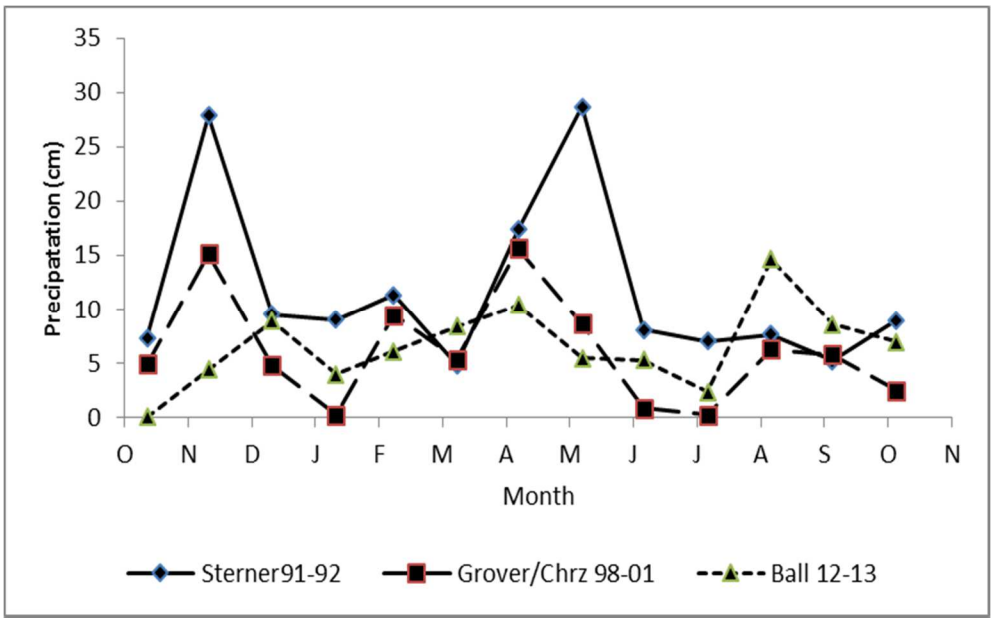

Figure 4.3 Monthly total precipitation in cm during the study periods of Sterner (1994), Grover and Chrzanowski (2005), and the present study. Data are compiled from the National Oceanic and Atmospheric Administration station 13960 Dallas Love Field Airport.

water temperatures ranged from 6.5 °C to 19.8 °C and water masses were well-mixed (Figure 4.4; Figure 4.5; Figure 4.6). Minimum water temperatures of 6.5 °C were observed in January 2013 (Figure 4.4; Figure 4.5; Figure 4.6).

The water column stability (E) m^{-1} was calculated using the vertical density gradient normalized by the density (ρ) with the following equation:

$$E=-\frac{1}{\rho}\frac{d\rho}{dz} \quad (1)$$

where z denotes the depth in meters. Stability was defined to be positive if E > 0 whereas the water mass was instable if E< 0 based on a typical observational error of E = ±4.2 x 10^{-5} m^{-1} for the lake. Any value within the observational error has been assumed to be neutral stable (E=0). The observational error in stability (E = ±4.2 x 10^{-5} m^{-1} for the lake) was determined by calculating the relative change by the instrumental error of ±0.2 °C for a reference temperature of 20°C, resulting in a density error of ±0.042 Kg m^{-3}. Any water mass with a stability of E= ±4.2 x 10^{-5} m^{-1} thus assumed to be neutral stable (Table 4.1).

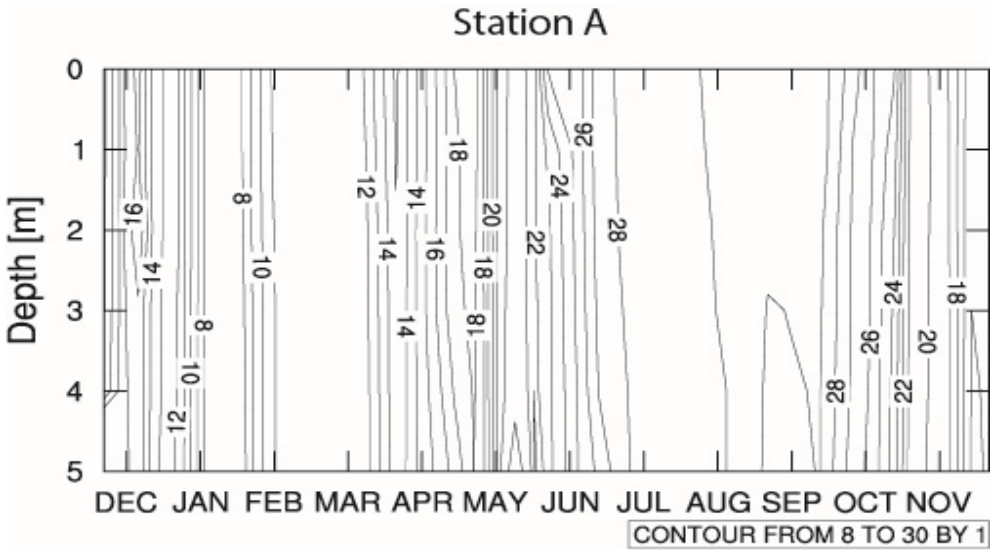

Figure 4.4 Hovmöller diagram of temperature for November 2012 to November 2013 in Joe Pool Lake at site A. Depths given as meters below the surface and are not corrected for variations in lake elevations.

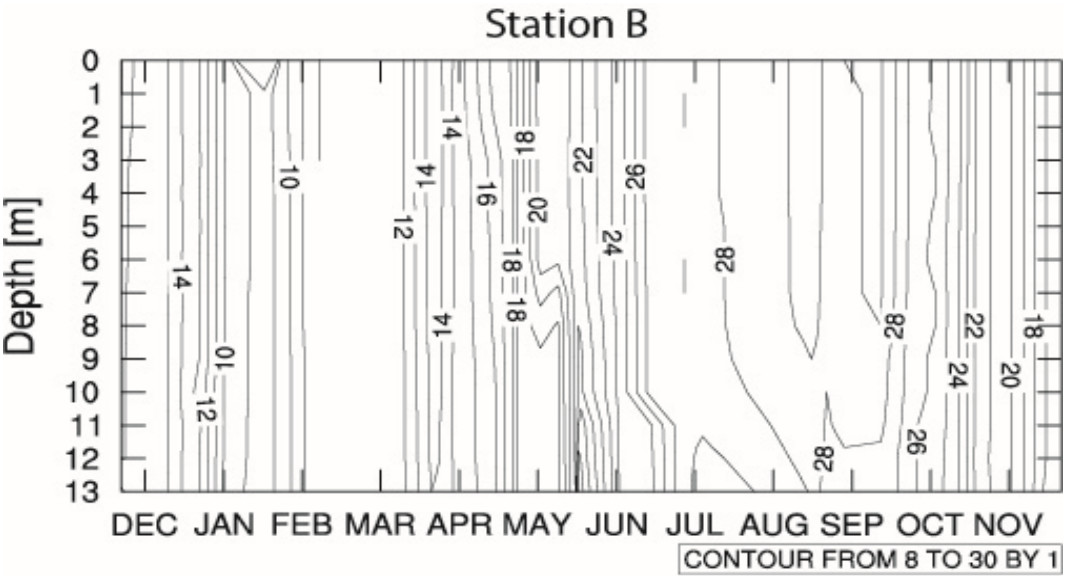

Figure 4.5 Hovmöller diagram of temperature for November 2012 to November 2013 in Joe Pool Lake at site B. Depths given as meters below the surface and are not corrected for variations in lake elevations.

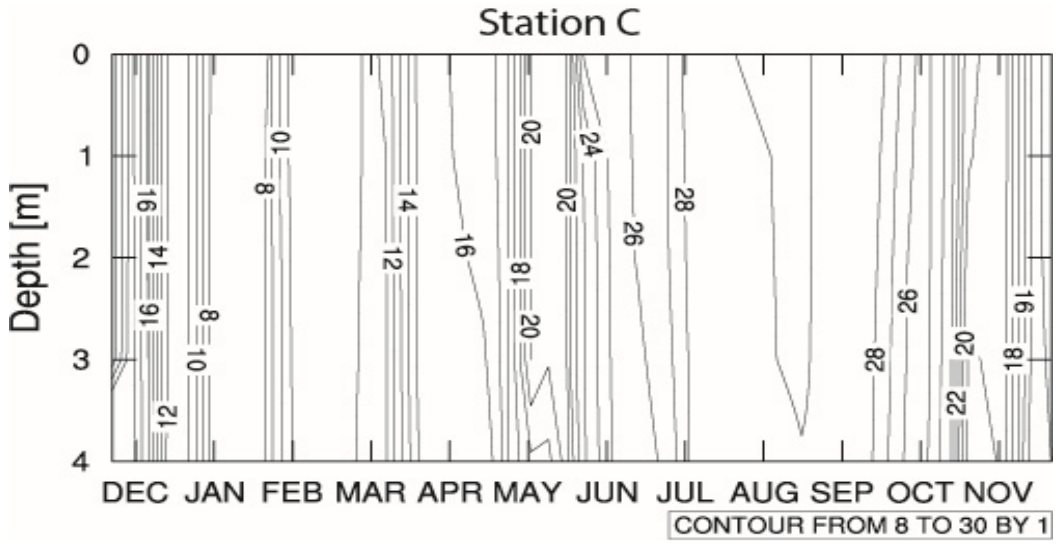

Figure 4.6 Hovmöller diagram of temperature for November 2012 to November 2013 in Joe Pool Lake at site C. Depths given as meters below the surface and are not corrected for variations in lake elevations.

Table 4.1 Stability with depth from November 2012 through November 2013 for site B. (BLUE = + positive, RED = - negative, and WHITE = N neutrally stable; see eq. 1)

Depth	Nov.	Dec.	Jan.	Feb.	Mar.	Apr.	May	Jun.	Jul.	Aug.	Sep.	Oct.	Nov.
0	N	N	N	N	N	N	N	N	N	N	N	N	N
0.5	N	N	-	N	N	N	N	N	N	N	N	N	-
1	N	N	N	N	N	N	N	N	N	N	N	N	N
1.5	N	N	N	N	N	N	N	N	N	N	N	N	N
2	N	N	N	N	N	N	N	N	-	N	N	N	N
2.5	N	N	N	N	N	N	N	N	N	N	N	N	N
3	N	N	N	N	N	N	N	N	N	N	N	N	N
3.5	N	N	N	N	N	N	N	N	N	N	N	N	N
4	N	N	N	N	N	N	N	N	N	N	N	N	N
4.5	N	N	N	N	N	N	N	N	N	N	N	N	N
5	N	N	N	N	N	N	N	N	N	N	N	N	N
5.5	N	N	N	N	N	N	N	N	N	N	N	N	N
6	N	N	N	N	N	N	+	N	-	N	N	N	N
6.5	N	N	N	N	N	N	+	N	N	N	N	N	N
7	N	N	N	N	N	N	+	N	N	N	N	N	N
7.5	N	N	N	N	N	N	+	N	N	N	N	N	N
8	N	N	N	N	N	N	+	N	N	N	+	N	N
8.5	N	N	N	N	N	N	N	N	N	N	+	N	N
9	N	N	N	N	N	N	N	N	N	+	N	N	N
9.5	N	N	N	N	N	N	N	N	N	N	N	N	N
10	N	N	N	N	N	N	+	+	-	+	N	N	+
10.5	N	N	N	N	N	N	+	+	-	+	N	N	N
11	N	N	N	N	N	N	+	N	-	N	+	+	N
11.5	N	N	N	N	N	N	+	N	-	N	N	+	N
12	N	N	N	N	N	N	N	N	-	+	N	-	N
12.5	N	N	N	N	N	N	N	N	-	+	N	-	N
13	N	N	N	N	N	N	N	N	N	+	N	N	N

The water column at site B was generally near-neutrally stable throughout the winter months (Table 4.1). Dissolved oxygen concentration in the reservoir was maximal during the winter season (13.6 mol L^{-1} O_2) and generally uniform throughout the water column due the near-neutral stability, although an anomalous decrease in dissolved oxygen occurred near the lake bed at site C, for example on February 2, 2013 (Figure 4.7; Figure 4.8; Figure 4.9). Dissolved oxygen saturation [O_{2sat}] was calculated using the Weiss (1970) equation:

$$[O_{2sat}] = \frac{[O_{2obs}]}{[DO]} * 100 \quad (2)$$

where

$$[DO] = DO_0 * F_S * F_P \quad (3)$$

and

$$DO_0 = 1.42905 \exp\left[-173.4292 + 249.6339\left(\frac{100}{T}\right) + 143.3484\left(\ln\left(\frac{T}{100}\right)\right) - 21.8492\left(\frac{T}{100}\right)\right] \quad (4)$$

and

$$F_S = \exp\{S * [-0.033096 + 0.014259\left(\frac{T}{100}\right) - 0.0012000\left(\frac{T}{100}\right)^2]\} \quad (5)$$

and

$$F_P = \frac{P-u}{760-u} \quad (6)$$

DO_o is the baseline concentration of dissolved oxygen in mg L^{-1} of fresh water, Fs is the salinity correction factor, and Fp denotes the pressure correction factor (Weiss 1970) with *T* in temperature in Kelvin, *S* is salinity in parts per thousands, *P* is the barometric pressure in mm Hg, and *u* is the vapor pressure of water in mm Hg. During this period oxygen saturation never dropped below 90% saturation and the upper half of the water column was often supersaturated (results not shown). This anomaly was

verified with a spike in NH_4 measured on the same day. Secchi disk depths, reaching a minimum value of 0.3 m during this season, was insignificantly correlated to precipitation (Figure 4.10; Table 4.2). Soluble reactive phosphorus (SRP) is higher during these colder months with a significant peak on November 6th of 2013 (Figure 4.11). Total phosphorus (TP) concentrations did not follow this trend in 2012 (Figure 4.12). Dissolved inorganic nitrogen (DIN) during the winter months varied between the sampling sites. The highest DIN concentration measured during this period was 11.0 µmol l^{-1} at site C on January 16, 2013; site A was also found to have a peak on January 6, 2013 of 10.9 µmol l^{-1} (Figure 4.13). At site B however the peak was smaller with a concentration of 4.6 µmol l^{-1} on February 27, 2013 (Figure 4.13). November and December DIN concentrations were depleted. Correlation between precipitation and Secchi disk depth and nutrient data were inconclusive (Table 4.2).

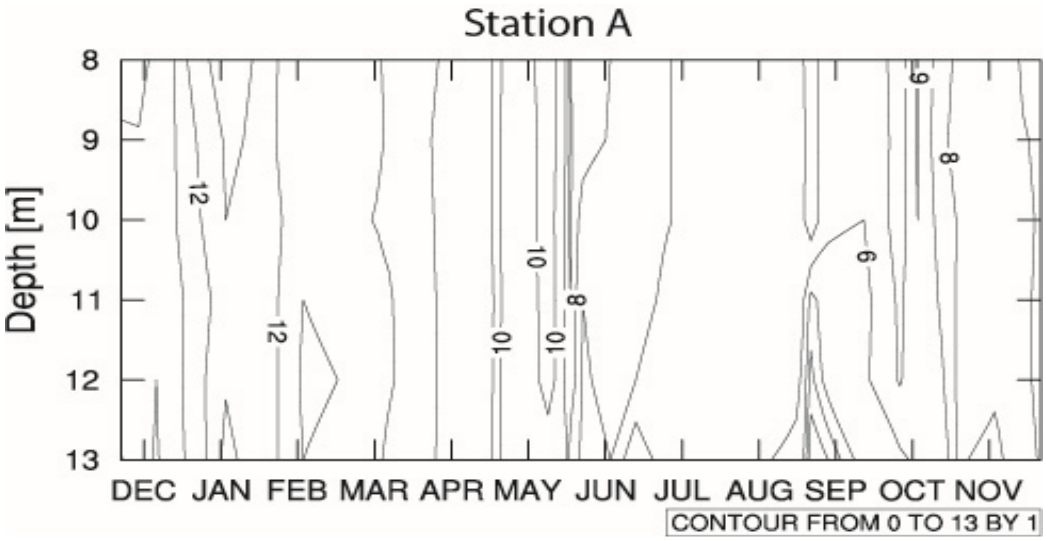

Figure 4.7 Hovmöller diagram of dissolved oxygen mg L^{-1} for November 2012 to November 2013 in Joe Pool Lake at site A. Depths is given in meters below the surface and are not corrected for variations in lake elevations.

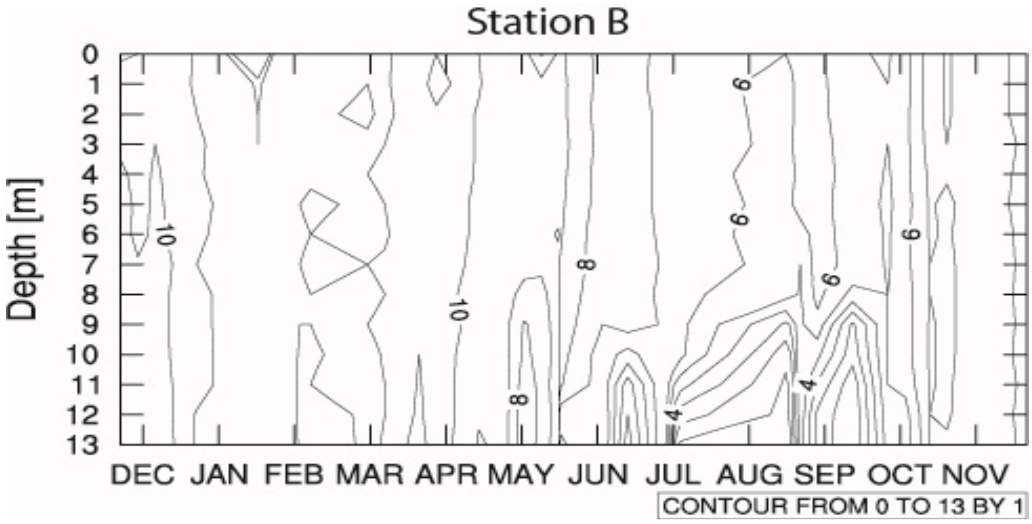

Figure 4.8 Hovmöller diagram of dissolved oxygen mg L^{-1} for November 2012 to November 2013 in Joe Pool Lake at site B. Depths is given in meters below the surface and are not corrected for variations in lake elevations.

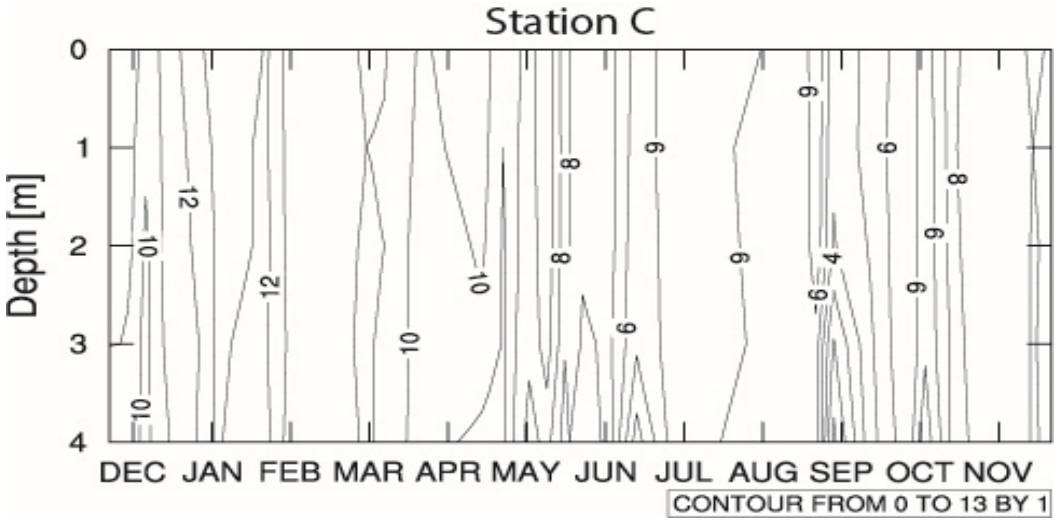

Figure 4.9 Hovmöller diagram of dissolved oxygen mg L^{-1} for November 2012 to November 2013 in Joe Pool Lake at site C. Depths is given in meters below the surface and are not corrected for variations in lake elevations.

During spring (March-May) winds ranged between 4.7 m s^{-1} and 5.0 m s^{-1}, which was higher than in the other seasons (Figure 4.2). Moderate temperatures during spring were between 13.1 °C and 22.2 °C (Figure 4.1). Precipitation was relatively high with a

peak of 10.4 cm in May (Figure 4.3). The lake was well-mixed until May when stratification increased due to increased solar radiation (Figure 4.14). Lake surface temperatures in spring transitioned from cooler, as low as 10.9 °C, water masses to much warmer water masses, as high as 25.4°C (Figure 4.4; Figure 4.5; Figure 4.6).

The reservoir was neutrally stable during both March and April but fluctuated between neutrally and positively stable in May (Table 4.1). Dissolved oxygen concentrations followed a similar trend with maximal values of 11.9 mg L^{-1} occurring in March and decreasing through May to 5.4 mg L^{-1} in the bottom waters as stratification increased (Figure 4.7; Figure 4.8; Figure 4.9). Dissolved oxygen was supersaturated in the mixed layer and under saturated (49.8 %) below the thermocline. Secchi disk depths were

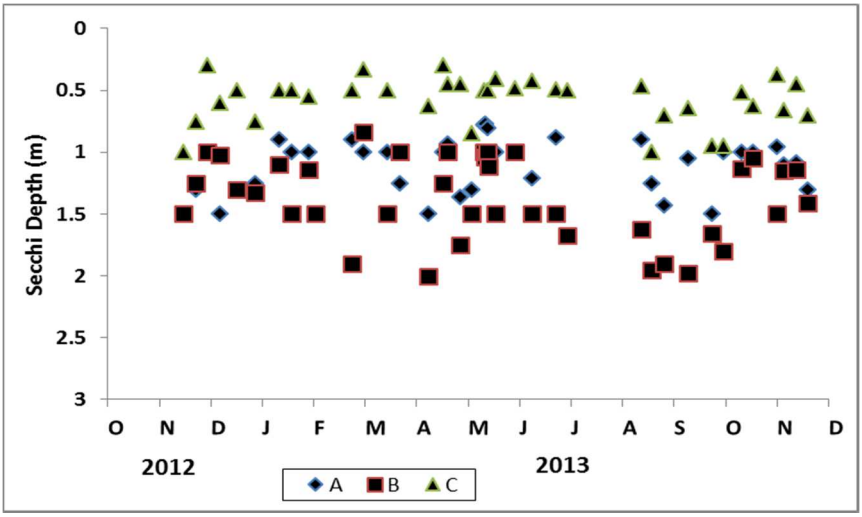

Figure 4.10 Secchi disk depths for November 2012 to November 2013 in Joe Pool Lake at sites A (blue diamond), B (red quadrangle), and C (green triangle).

maximal during the spring months ranging from 0.3 m occurring at site C to 2.0 m occurring at site B while SRP concentrations were depleted (Figure 4.10; Figure 4.11). DIN concentrations were highest in the spring months with the highest concentration of 26.8 µmol L^{-1} and TP was highest in May for all three sampling locations (Figure 4.13,

Figure 4.12). High amount of precipitation in spring was significantly inversely correlated to Secchi disk data and correlated to TP. Correlation of rainfall with other tracers were inconclusive (Table 4.2).

Table 4.2 Secchi depth and nutrient correlation to precipitation throughout winter (DJF), spring (MAM), summer (JJA) and fall (SON). Only values in bold were found to be significant ($p \leq 0.07$).

Parameter	A				B				C			
Site	DJF	MAM	JJA	SON	DJF	MAM	JJA	SON	DJF	MAM	JJA	SON
Secchi	-0.49	**-0.73**	-0.15	**0.64**	-0.12	-0.38	-0.27	0.09	0.01	-0.31	-0.13	0.46
SRP	0.50	0.13	0.35	-0.09	-0.32	-0.53	0.11	-0.17	-0.31	**-0.64**	-0.25	0.00
TP	**0.90**	**0.81**	0.28	0.15	0.07	-0.05	-0.11	-0.24	0.37	-0.34	0.07	-0.24
NO_2	-0.21	0.28	0.13	-0.18	0.23	0.36	-0.24	-0.24	0.69	0.51	0.21	-0.04
NO_3	**0.93**	-0.37	0.47	0.42	0.14	0.09	0.53	-0.24	0.68	0.25	-0.30	0.04
NH_4	-0.13	-0.47	0.32	**0.98**	0.37	-0.28	0.24	**0.63**	0.14	0.03	0.30	-0.12
SRSi	0.05	-0.17	**-0.83**	0.58	-0.16	-0.01	-0.20	-0.02	-0.16	0.18	-0.55	0.03

During the summer (June-August) surface air temperatures was highly variable ranging from 19.0 °C to 30.1 °C with maximal surface air temperatures of 30.1 °C in August 2012 (Figure 4.1). Wind speeds during this time were the lowest of this study ranging from 2.6 m s^{-1} to 3.7 m s^{-1} (Figure 4.2). Water temperatures were high range from 30 °C to 18.7 °C with intermittent stratification till mid-June (Figure 4.4; Figure 4.5; Figure 4.6). Stratification during summer at site B caused depletion of dissolved oxygen in deeper layers with decreased saturation of dissolved oxygen to 9.65% on July 3, 2013 (Figure 4.7; Figure 4.8; Figure 4.9; Table 4.1). Surface SRP remained depleted throughout these months (Figure 4.11). Values of DIN during the summer are lower than in other than in other seasons. TP was not depleted during the summer months, the lowest measured concentration occurred during this time period (Figure 4.12, Figure 4.13). Secchi disk

depths ranged from 0.42 m to 1.98 m with Secchi depths increasing in mid-August (Figure 4.10). Correlation calculations between precipitation and nutrient concentrations produced inconclusive results (Table 4.2). During fall (September-November) stratification declined in the reservoir to near-neutral conditions with water temperatures ranging from 29.1 °C to 13.2 °C (Figure 4.4; Figure 4.5; Figure 4.6; Table 4.1). The highest amount of precipitation (147 mm) occurred during fall in September 2013 (Figure 4.3), related to a blocked low pressure system over North Central Texas. Dissolved oxygen concentrations ranged from 11.9 mg L^{-1} to anomaly of 0.03 mg L^{-1}, which occurred on September 11, 2013 (Figure 4.7; Figure 4.8; Figure 4.9). Dissolved oxygen was generally well saturated except for bottom waters in September, which averaged 11% lower than the surface values. Surface air temperatures during this period displayed the largest variability for the year, ranging from 11.0 °C to 27.0 °C.

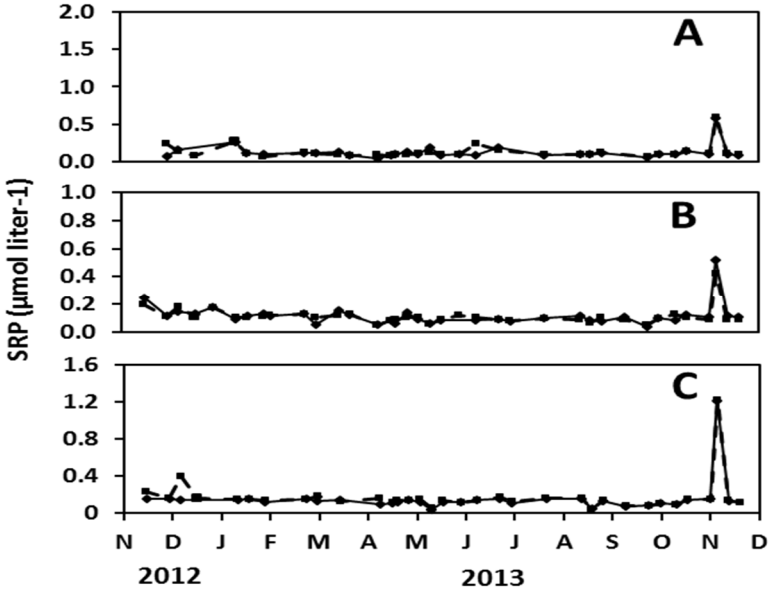

Figure 4.11 Concentrations of soluble reactive phosphorus (SRP) for 0.5-m depth samples (solid line) and average of samples from entire water column (dashed) for sites A, B, and C.

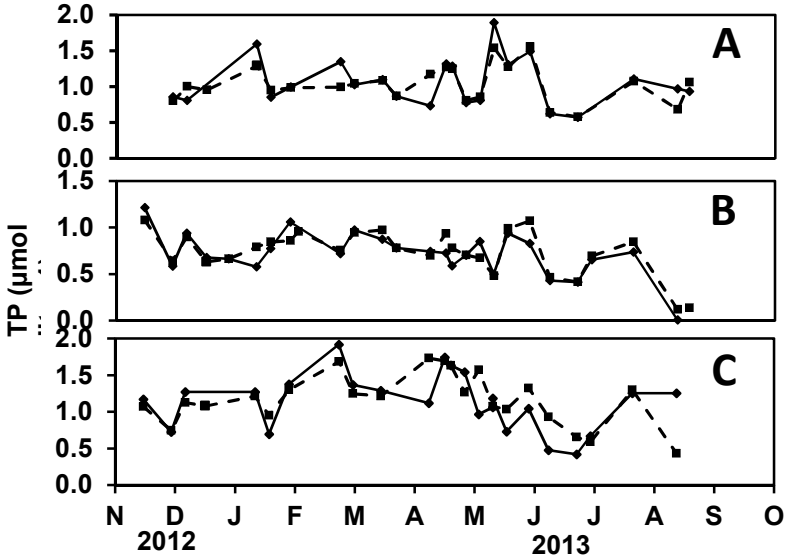

Figure 4.12 Concentrations of total phosphorus (TP) for 0.5-m depth samples (solid line) and average of samples from entire water column (dashed) for sites A, B, and C.

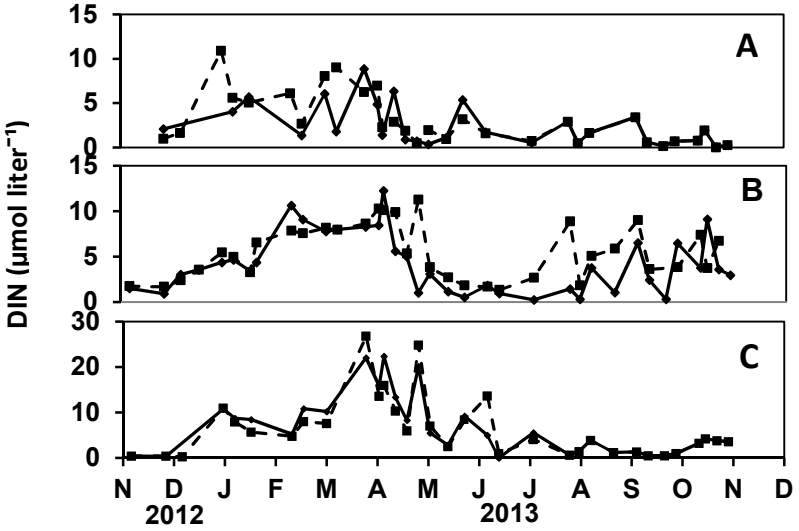

Figure 4.13 Concentrations of dissolved inorganic nitrogen (DIN) for 0.5-m depth samples (solid line) and average of samples from entire water column (dashed) for sites A, B, and C.

Wind speeds reached maximum values of 3.8 m s^{-1} (Figure 4.1; Figure 4.2). Secchi disk depths were between 1.98 m and 0.37 m (Figure 4.10). During this period DIN concentrations increased during the fall season from nearly depleted values during summer months (Figure 4.13). Analysis of observed TP concentrations during the fall of 2013, revealed large uncertainties in the measurements that ranged from 0.8 µmol L^{-1} to 1.2 µmol L^{-1} during the fall season (Figure 4.12). SRP concentrations, however, were complete and ranged from 0.04 µmol mg L^{-1} to 1.2 µmol mg L^{-1} (Figure 4.11). The largest concentration of SRP measured during this study occurred on November 6th of 2013. A positive correlation was found between precipitation and Secchi disk depth at site A and with NH_4 at sites A and B (Table 4.2).

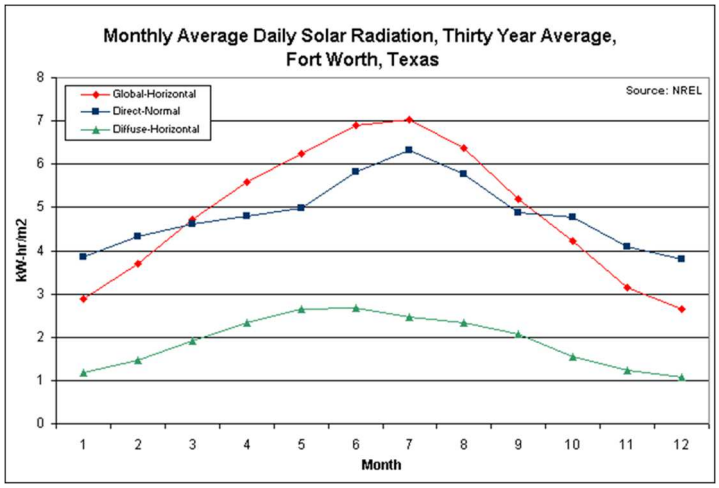

Figure 4.14 Monthly average for over thirty years of daily solar radiation in Fort Worth, Texas shown in KW-hr/m^2 (data from NREL;http://www.me.utexas.edu/~solarlab/FortW.html).

4.2. Long-term Seasonal Variations

Monthly air temperature data suggests possible long-term increase of approximately 2.8°C from Sterner (1994) to this study (Figure 4.1). Variation between

Grover and Chrzanowski (2004) and this study shows a small 0.03 °C increase in the minimum air temperature and a 1.36°C decrease in the maximum air temperature (Figure 4.1). Precipitation has decreased from the Sterner's (1994) study to this study with the maximum decreasing from 28.7 cm in 1992 to 14.7 cm in 2013 (Figure 4.3), partially due to a decrease in the natural aerosol load in the northern hemisphere from the Mt. Pinatubo eruption in 1991 (Figure 4.15; Kirchner et al. 1999), and partially due to climate change and variability. Wind speed and direction is not available for Sterner (1994), but these data are available in the study of Grover and Chrzanowski (2004). The available data suggest that wind speeds during the 1998 to 1999 study were more variable than those from 2012 to 2013, potentially due to higher thunder storm frequency during a La Niña year, but the wind direction is consistent between records with winds from the Northeast during winter month and transitioning to winds from the Northwest during the summer months (Figure 4.2). Secchi disk depth variation between the 1991 to 1992 study and the 2012 to 2013 study is substantial (Figure 4.10; Figure 4.16).

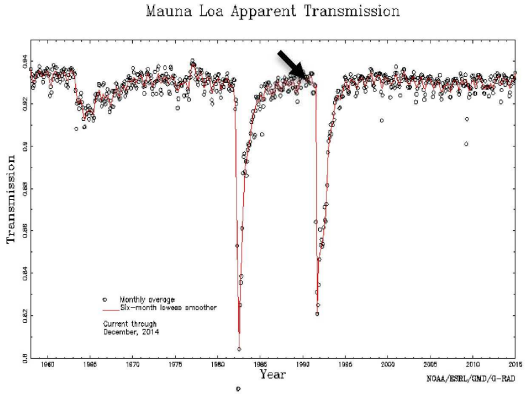

Figure 4.15 The "apparent" transmission, or transmission ratio (Ellis and Pueschel, 1971), is derived from broadband (0.3 to 2.8um) direct solar irradiance observations at the Mauna Loa Observatory (19.533 ° N, 155.578 ° W, elev. 3.4 km) in Hawaii. The arrow indicates the time of the occurrence of the Mt. Pinatubo eruption. Data are for clear-sky mornings between solar elevations of 11.3 and 30 degrees. The plotted points are monthly averages and the plotted curve results from a 6 month Lowess statistical smoother (NAOO http://www.esrl.noaa.gov/gmd/grad/mloapt.html, 2014).

The Sterner (1994) data depicts pre-flood and post-flood periods within the reservoir with the highest Secchi disk depth being 2.5 m at site B and the lowest Secchi disk depth that is less than 0.5 m at site C due to increased turbidity caused by a reservoir flooding by enhanced rainfall and associated particle transport (Figure 4.16). During this study variation in the lake's particle concentration was insignificant and the maximum Secchi disk depth was 1.95 m at site B; though there is evidence of two small events that increased Secchi disk depths one in April and the other in August (Figure 4.10). The August event coincided with the lowest wind speeds of the year (Figure 4.2). Observations from Sterner (1994) and this study both found that site B generally has the highest Secchi disk depth and site C has the lowest.

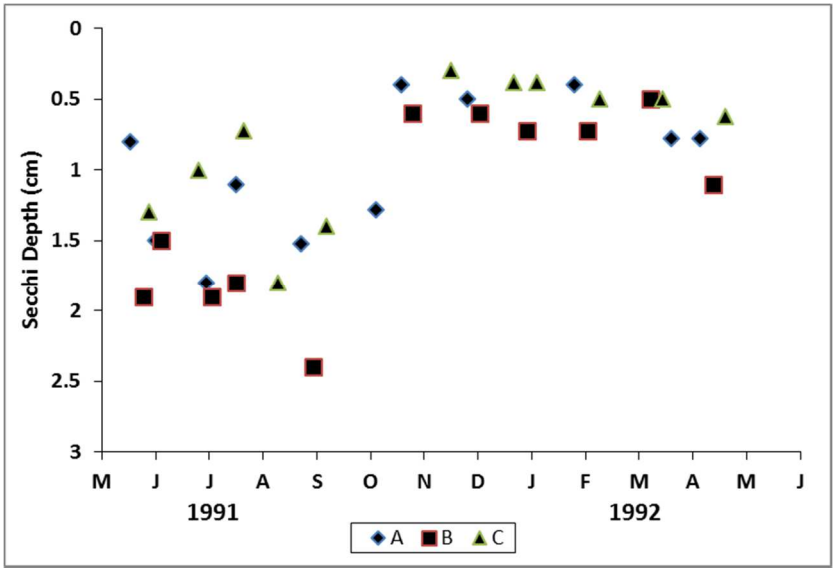

Figure 4.16 Secchi disk depths beginning in 1991 from Sterner (1994). Figure adapted from Sterner (1994).

Temperature and oxygen mixing throughout the water column in both study periods depict complete mixing during winter months and increased stratification during the summer months (Figures 4.4-4.9; Figure 4.17). During this study there is also

occurrence of oxygen depletion at site C in February at the lake bottom (Figure 4.9). Sterner (1994) found site B to have a distinct thermocline from June to late September, and this study found that a distinct thermocline appeared at the beginning of May and continued intermittently mixing events till the middle of June (Figure 4.17; Figure 4.5). Sites A and C showed the same trends with smaller durations of stratification events for both temperature and oxygen (Figure 4.4; Figure 4.5; Figure 4.17; Figure 4.7; Figure 4.9). Water temperatures ranged from approximately 8°C to 30°C in 1991 to 1992 and 4.3°C to 29.4C in 2012 to 2013 (Figure 4.17; Figure 4.4; Figure 4.5; Figure 4.6).

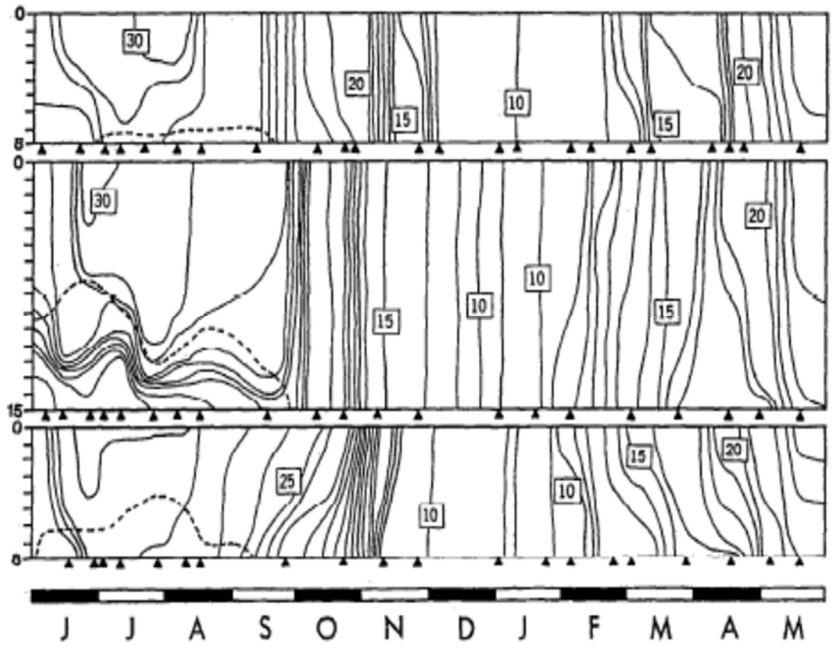

Figure 4.17 Hovmöller diagram (time and depth) of temperature at sites A (top), B (middle), and C (bottom). Isotherms every °C; dashed lines denote the 1mg O_2 L^{-1} isopleth from 1991 to 1992. Depth given as meters below surface. Numbers not corrected for changes in lake level (Sterner 1994).

Comparing SRP concentrations from this survey and a study in 1991 (Sterner, 1994) indicates a negative trend in the SRP concentration of Joe Pool Lake. In 1991,

October and March SRP concentrations increased to as much as 1.5 µmol L^{-1} but were very low throughout the rest of the year (Figure 4.18). During 2000 survey of the lake (Grover and Chrzanowski, 2004), SRP concentrations were low throughout the year, with the maximum of 0.4 µmol L^{-1} (Figure 4.19). During this study, SRP concentrations were similar to those of 2000, with low concentrations throughout the year and with a small negative trend during the spring and early summer months and one peak of 1.22 µmol L^{-1} that occurred on November 6th of 2013 potentially due to a cumulative rainfall of ~3.1 cm over a period of three days from November 4th through the 6th (Figure 4.11; Figure 4.3).

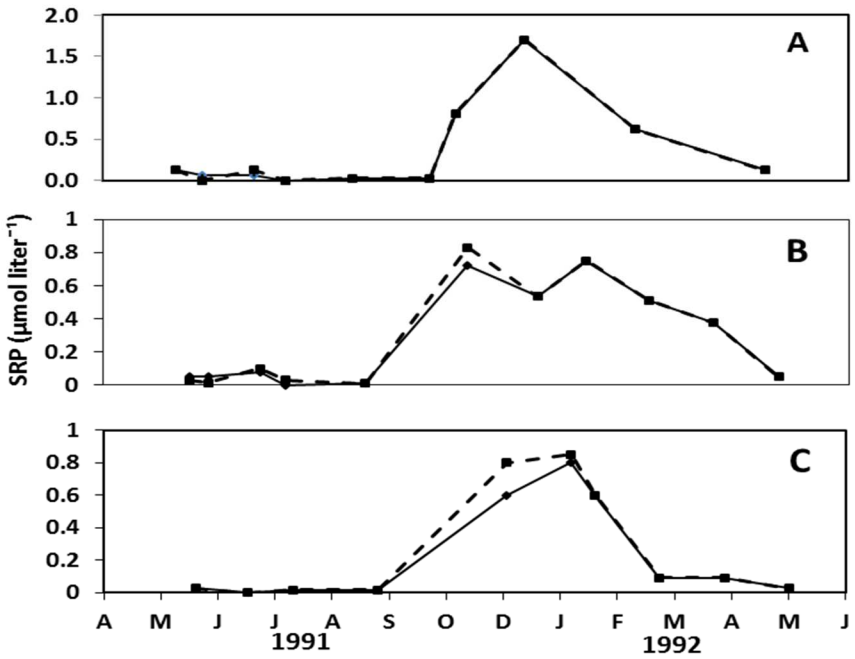

Figure 4.18 Concentrations of soluble reactive phosphorous (SRP), beginning in 1991, for 2-m depth samples (solid line) and depth-integrated samples (dashed) for sites A, B, and C (Sterner 1994).

In both this study and Grover and Chrzanowksi (2004), nitrogen is given as DIN however in Sterner (1994) nitrogen is measured as nitrate. All three studies depict

lower concentrations during the summer months and higher concentrations throughout the rest of the year. The concentration of nitrogen during the three visits however has decreased since 1991 and 1999 but the concentrations in 2000 are similar to those of this study (Figure 4.20; Figure 4.19; Figure 4.13).

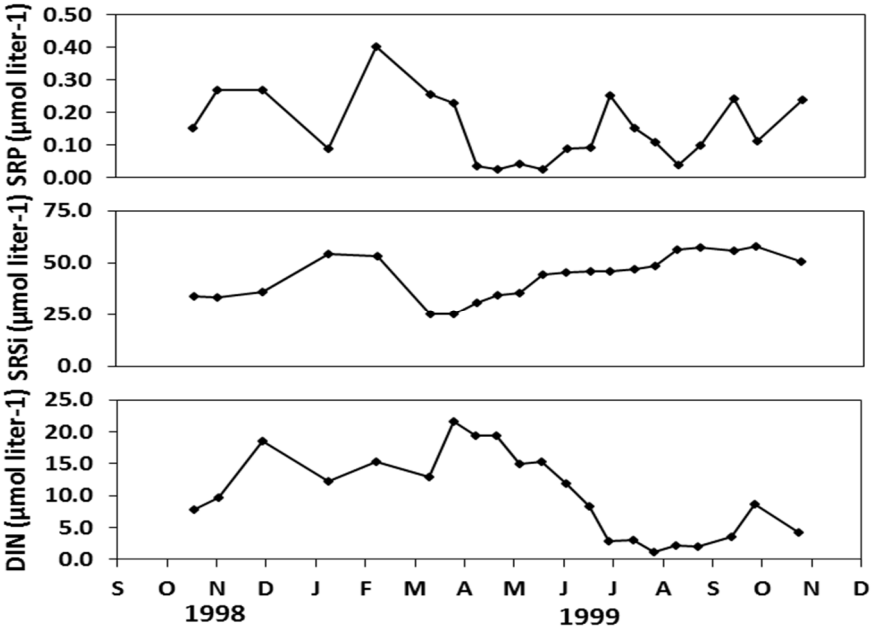

Figure 4.19 Nutrient concentrations of SRP, SRSi, and DIN from integrated samples near the dam near site B, beginning in 1998 (Grover and Chrzanowski 2004).

A SRSi comparison indicates lower concentrations of silicate in this study. Since Sterner (1994) SRSi concentrations have decreased from a high of approximately 120 µmol L^{-1} to a low of 49.2 µmol L^{-1} in 2013 (Figure 4.13; Figure 4.21; Figure 4.22). Fluctuations in SRSi concentrations coincided with precipitation throughout the year for all three studies.

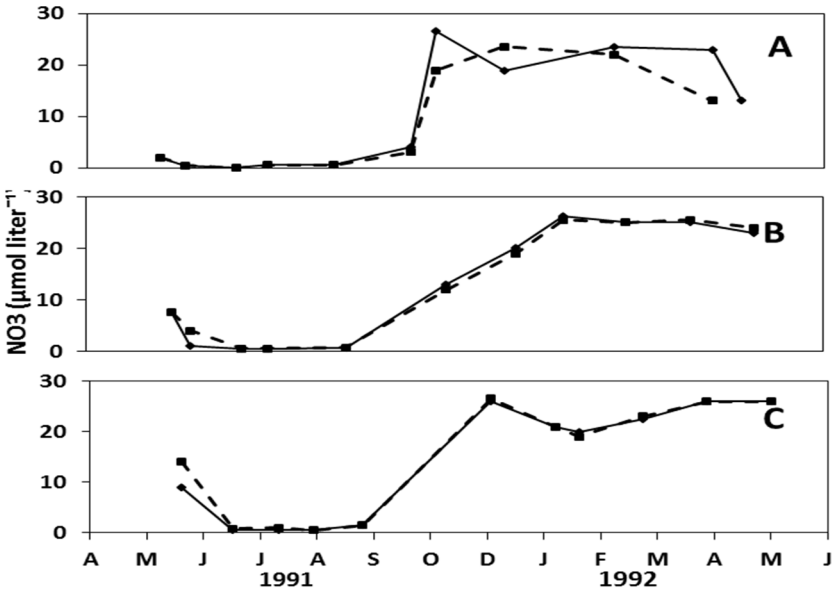

Figure 4.20 Concentrations of soluble reactive NO_3, beginning in 1991, for 2-m samples (solid line) and depth-integrated samples (dashed) for sites A, B, and C (Sterner 1994).

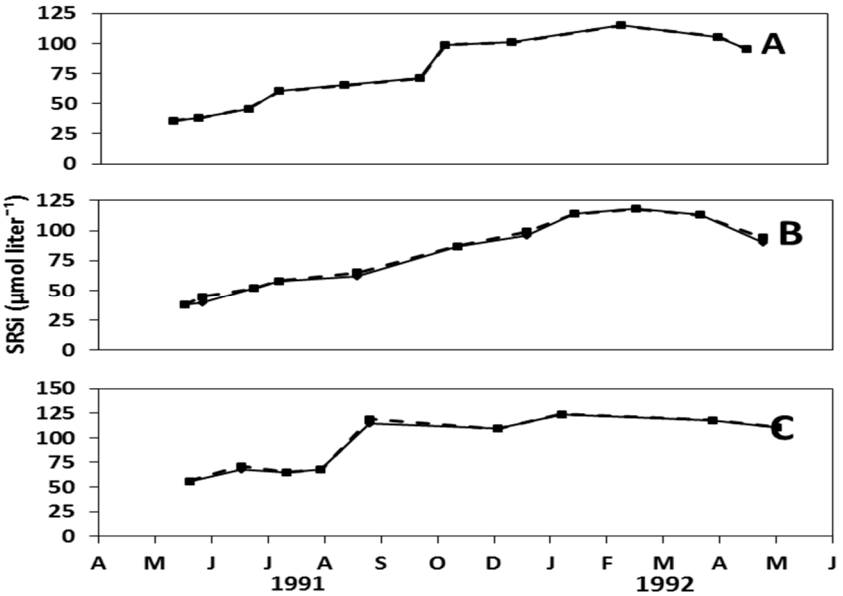

Figure 4.21 Concentrations of soluble reactive SRSi, beginning in 1991, for 2-m samples (solid line) and depth-integrated samples (dashed) for sites A, B, and C (Sterner 1994).

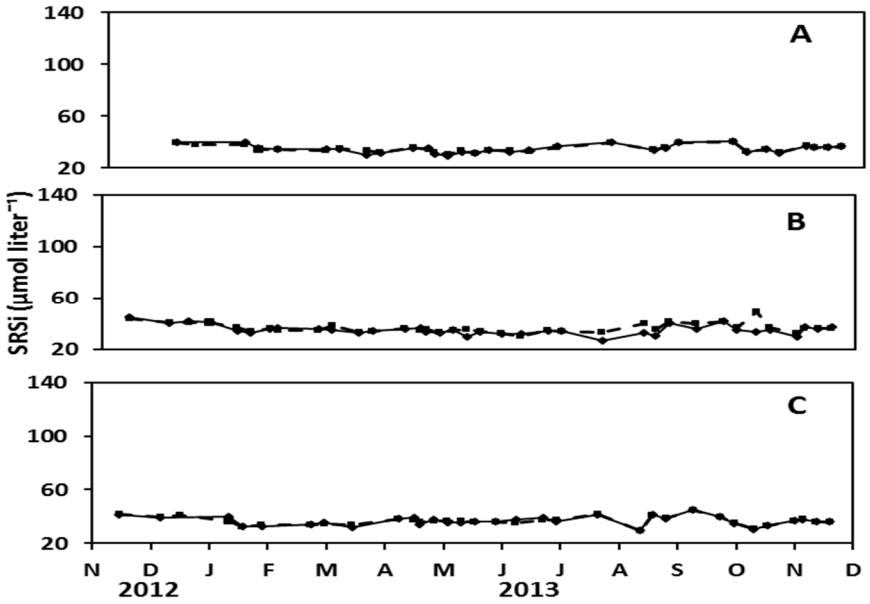

Figure 4.22 Concentrations of SRSi for 0.5-m samples (solid line) and average of samples from entire water column (dashed) for sites A, B, and C.

Chapter 5

Discussion

5.1 Seasonal variations during 2012 and 2013

The increased monthly air temperatures accompanied by lower precipitation are likely, particular during the 2011-2014 Texas drought which has likely been intensified by the negative phase of ENSO in 2011 (Nieslen-Gammon 2012) and the positive phase Atlantic Multidecal Oscillation that began in 1996 (AMO; Schlesinger and Ramankutty 1994; http://www.esrl.noaa.gov/psd/data/correlation/amon.sm.data). Changes in ENSO had a significant influence on seasonal variance within the reservoir. While this study occurred during a neutral ENSO period, the survey of Sterner (1994) in 1991 through 1992 occurred during an El Niño year, whereas the survey of Grover and Chrzanowski (2004) occurred during a La Niña year in1998 through 1999 (Figure 5.1). Wind speed over Joe Pool Lake may also have increased by other climate variations like the Interdecadal Pacific Oscillation (IPO) shifting from a positive phase to a negative phase in 2000 (England et al. 2014).

In the winter and late fall, low solar insolation (Figure 4.14), cold temperatures due to outbreak of cold arctic air masses, and mean wind speed > 4 m s^{-1} produce convective and wind-induced mixing (Figure 4.2). This mixing decreases water temperatures throughout the lake as well as increases the dissolved oxygen concentrations due to higher solubility and reduced biological pump (Volk and Hoffert 1985). SRP, TP, and DIN concentrations during this period were affected by atmospheric deposition, temperature and light limitation of biological productivity, and with little influence from runoff from precipitation. For example, the largest peak SRP concentration on November 6th, 2013 was likely due to high winds induced deposition and increased

cloud cover that reduced photosynthetic productivity. The increase in turbidity was likely due to increased particle concentration, as well as, the wind speed cause the decrease in the Secchi disk depth (Figure 4.10).

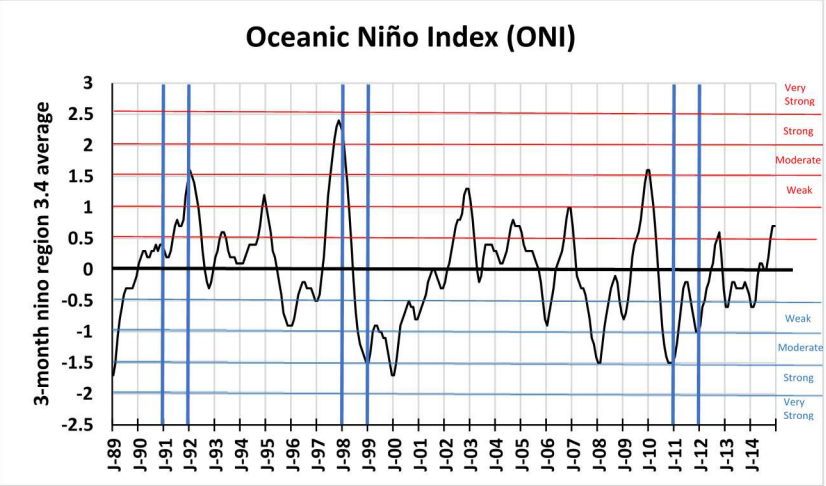

Figure 5.1 El Niño index for the average El Niño region 3 and 4. Red denotes strong El Niño, blue denotes La Niña, and black are El Niño neutral conditions. Blue lines indicate study periods (http[://www.cpc.ncep.noaa.gov/products/ analysis_monitoring/ensostuff/ensoyears.shtml)

During spring surface air temperatures were increasing in response to higher solar radiation. Strong air surface temperature gradients and associated intense pressure difference linked to differential heating of Gulf of Mexico water masses and south-central U.S. land masses lead to high winds speeds >4.5 m s^{-1} (Figure 4.2). During the summer, the increase in solar radiation and rise in air temperatures caused an increase in lake surface temperatures and enhanced thermally-stratified conditions (Figure 4.1; Figure 4.5). This stratification occurred when the potential energy due to the stability by the vertically temperature gradient is larger than the wind-induced turbulent mixing (Boehrer and Schultze 2008). Dissolved oxygen depletion was likely caused by reservoir stratification, decreased solubility and increased respiration by enhanced microbial

activity with the warming. As stratification occurred, dissolved oxygen in the lake's bottom water near the lake floor was no longer being ventilated by surface waters and thus became depleted. Increased phyto- and zooplankton population and associated higher turbidity led to a rise Secchi depth during this period. The depletion of SRP during this period is evidence of nutrient depletion due to productivity. DIN and TP were not depleted possibly due to the increase in run off from fertilizers, as well as the release of phosphorus from sediment and NH_4 through decomposition, due to oxygen depletion at the reservoir floor.

Summer and early fall air temperatures were the highest air temperatures of this study and wind speeds were at the lowest. Stratification owing to high solar radiation, was intermittent due to perturbation by wind-induced mixing and from the input of cooler water through precipitation caused by thunderstorms and frontal systems. During August, concentrations of SRP and dissolved oxygen remain low with the lowest concentrations of oxygen in the study occurring during this time interval. Nutrient uptake by phytoplankton populations likely resulted in decreased DIN concentration, TP concentration, and Secchi disk depth. In September however, Secchi depth increased likely due to reduced rainfall and depleted nutrient concentrations limiting the growth of phytoplankton causing a decrease in the population.

5.2 Long term seasonal variations

Changes in temperature and precipitation throughout the three study periods are due to climate variations attributed to the volcanic eruptions, climate change, Dallas Fort Worth urban heat island, ENSO, and AMO. Sterner's (1994) survey was conducted during an El Niño year(1991-1992) with negative phase in the AMO, favoring cool conditions due increase in precipitation. This cooling trend could have been even more

amplified by the Mt. Pinatubo eruption in 1991 resulting in a significant increase in the aerosol concentration (Stenchikov et al. 1998, D'Aleo and Easterbrook 2010). Grover and Chrzanowski (2004) study in (1998-1999) occurred during a La Niña year (Smith et al. 2008; NCEP 2014), which led to warmer and drier conditions over North Central Texas. However, this study from 2012 to 2013 occurred during neither of these cycles. During this study, air temperatures were cooler than those of Grover and Chrzanowski (2004) and precipitation decline continuing drought conditions. Changes in ENSO and solar radiation also contributed to temperature and precipitation variations. In June of 1991 the volcanic eruption of Mount Pinatubo resulted in a sharp decline of solar radiation until 1995 and contributed to the lower temperatures recorded during that time period (Figure 4.16) (Kirchner et al. 1999; Stenchikov et al. 1998). Climate variations like the AMO could have also influenced the long-term environmental variations (Winguth and Kelp, 2013). Further, the long-term trend is likely caused by global climate change and intensified by the urban heat island of the Dallas Fort Worth metropolitan area (Winguth and Kelp, 2013).

During survey of Sterner (1994) Secchi disk depths values abruptly decreased due to flood events that occurred during the fall months whereas Secchi disk depths during this study are also affected by the construction of housing that is ongoing in the immediate drainage area. The reservoir dam accumulates fine grain particles deposited into Joe Pool Lake from runoff, wind and the additions of airborne particles from natural and anthropogenic sources. The effect of runoff on Secchi disk depth is most pronounce in spring and fall likely due to the increase rainfall and fertilizer use during spring and the increase in load that can occur in fall due to decreased ground cover as well as the decreased productivity within the reservoir. Decreased in Secchi disk depth is likely to continue due to continued drought causing decreased reservoir elevation further

concentrating entrained particles as well as through input of runoff during precipitation events (Figure 5.2; Figure 5.3; Figure 5.4). Rapid urban development over the drainage area of Joe Pool Lake together with reservoir aging likely caused a rise in turbidity and nutrient concentration due to increase use of fertilizers.

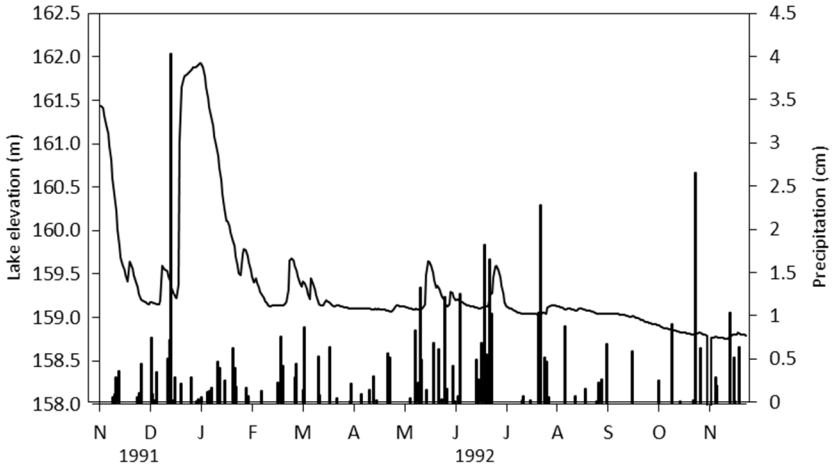

Figure 5.2 Daily lake elevation and precipitation for the period from November 1, 1991 through November 30, 1992 (Data supplied by United States Geological Survey and by the National Oceanic and Atmospheric Administration).

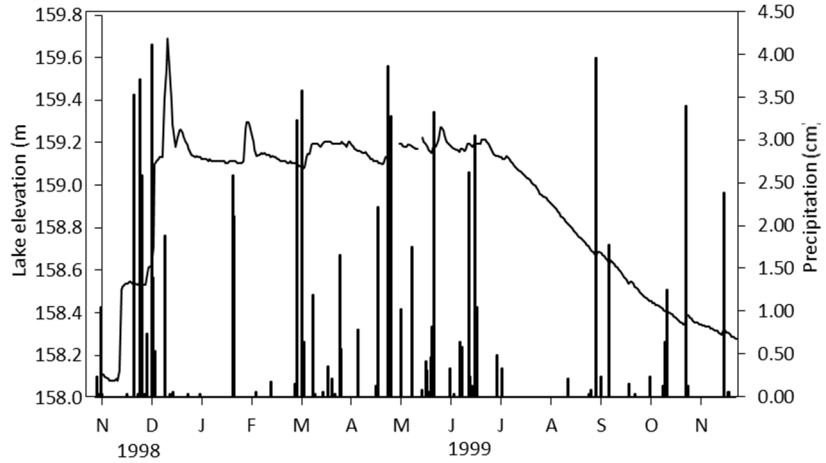

Figure 5.3 Daily lake elevation and precipitation for the period from November 1, 1998 through November 30, 1999 (Data supplied by United States Geological Survey and by the National Oceanic and Atmospheric Administration).

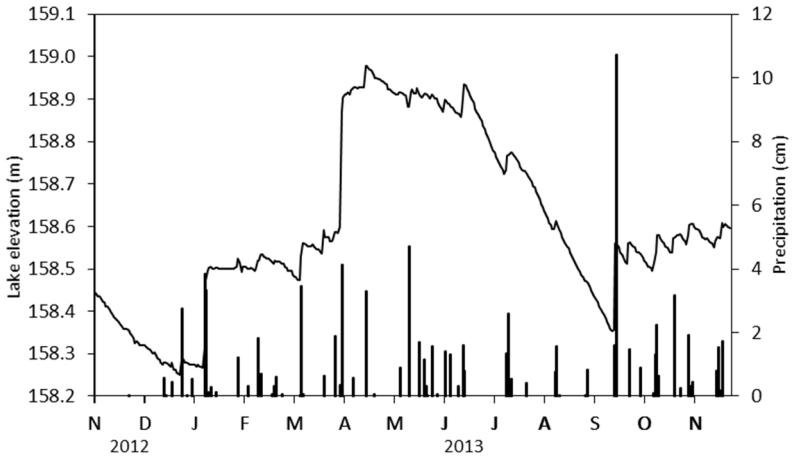

Figure 5.4 Daily lake elevation and precipitation for the period from November 1, 2012 through November 30, 2013. (Data supplied by United States Geological Survey and by the National Oceanic and Atmospheric Administration).

When compared, the oxygen and temperature profiles of the study periods of Sterner (1994) and this study suggest that the temporal variations in oxygen concentrations have not changed, with the exception of an anomalous low lake bed oxygen concentration during February of this study. The February anomaly cannot be explained at this time, although it has been confirmed with a measured peak in NH_4 on the same day. Temperature profiles from Joe Pool Lake during Sterner's (1994) study and this study both depict stratification only in the summer months and mixing throughout the year. Sterner (1994), however, found the summer stratification to be persistent over four months, while this study found stratification to occur earlier and intermittently over two months. The early onset of stratification is possibly due decreased input of cooler water though precipitation, and to increased surface warming due to higher air temperatures during the late spring and early summer months of this study. The early return to mixed conditions is likely due to higher precipitation in August that did not occur during the Sterner (1994) study. The inconsistency of stratification that occurred during this study is likely owing to the period of stratification occurring early during high winds.

Water temperature during this study were also slightly lower as well, which is a possibly cause for the difference in reservoir mixing. The lower water temperatures that occurred during this study are likely due to a cold weather event that occurred at the end of April causing a delay in summer temperature increased. Although some variation in lake mixing occurred between this and the Sterner (1994) study; the mixing regime of Joe Pool Lake remains the same. Joe Pool Lake is classified as discontinuous warm polymictic, when using the Lewis (1983) classification

Changes in nutrient concentrations through time, depicts decreasing nutrient concentration for SRP, DIN, and SRSi concentrations. Reservoir aging is likely the cause of the decline in the long-term changes in nutrients concentrations. The annual cycle of SRP and DIN cycle of this study is comparable to the study of Grover and Chrzanowski's (2004), the amplitude is lower compared to Sterner (1994). Lower concentrations of SRP and DIN during the summer are potentially linked increases in phytoplankton populations consuming available nutrients. Higher concentrations of SRP occur during the cooler periods owing to decreased phytoplankton, enhanced mixing, and river inflow from Mountain Creek and Walnut Creek due to precipitation. The recent evidence of the suppression of this cycle can be partly attributed to dry winter condition reducing the input of nutrients (Grover and Chrzanowski 2004). SRSi concentrations have also decreased through time but no discernable cycle has emerged. The decrease in nutrient concentrations from reservoir creation till now is likely due to the utilization of pre-impoundment terrestrial nutrients. As the preexisting nutrient load is utilized the reservoir is moving towards an aged and newly stable states.

Chapter 6

Future Outlook

The hydrological cycle is highly linked to climate variability and change as inferred from IPCC (2013), thus future work requires the understanding of impact of these changes on North Texas reservoirs. This study supported previous investigations' evidence that stratification, dissolved oxygen and nutrient distribution is altered remarkably by the climate fluctuations. Continued research of limnological processes is essential to preserve valuable resource for the environment and recreation. The importance of the effect of temperature on aquatic ecosystems should be further studied to help determine the impact of climate change, reservoir aging and continued urban development on the lake's environment.

Appendix A

Soluble Reactive Phosphate Analysis

Triplicate 50 ml aliquots of each sample and Milipore water, as well as, duplicate 50 ml aliquots of 1 µmol/liter, 2 µmol/liter, and 4 µmol/liter standards are put into acid-rinsed Wheaton bottles. 2 ml of acid-molybdate solution is added to each Wheaton bottle follow by the addition of 0.5 ml of ascorbic acid solution. The absorbance can then be measured with a spectrophotometer set at wavelength 720 nm after ten minutes using a 5 cm cuvette.

The standards for this analysis where made using a standard solution of 0.1380 g sodium phosphate monobasic monohydrate dissolved into 1000 ml of Milipore water. Using the standard solution, 1 ml was added to 1000 ml, 500 ml, and 250 ml to create standards of 1 µmol/liter, 2 µmol/liter, and 4 µmol/liter of phosphate. The standard solution can be refrigerated and stored for months, but the standards should be made on the day of analysis.

The acid-molybdate solution is made by slowly adding 144 ml of concentrated H_2SO_4 to 300 ml of Milipore water and cooling in an ice bath. When cooled dissolve 10 g of sulfamic acid, 12.5 g ammonium molybdate, and 0.34 antimony potassium tartrate into the solution. Once all the constituents of the reagent are dissolved bring the volume to 1000 ml with Milipore water. Store the acid-molybdate solution in an amber bottle and the solution is stable for months.

The ascorbic acid solution should be made on the day of use. To make the ascorbic acid solution, dissolve 10 g of ascorbic acid in 100 ml of Milipore water. Discard any unused reagent.

Appendix B

Total phosphorus

Triplicate 50 ml aliquots of each sample and Milipore water, as well as, duplicate 50 ml aliquots of 1 µmol/liter, 2 µmol/liter, and 4 µmol/liter standards are put into acid-rinsed Wheaton bottles. 8 ml of persulfate oxidation reagent is added to each bottle, the caps are placed loosely on, and the bottles are then autoclaved for 60 minutes set at a temperature of 121ºC. After autoclaving allow the bottles to cool to room temperature and then filter using 0.45µm cellulose filters. Once filtered the samples are corrected to a pH of approximately 8.3 by first adding one drop of phenolphthalein indicator, then 6N NaOH is added drop by drop until the sample turns pink, and to complete the correction 10% HCl is added drop by drop till the sample is once again clear. After these steps are completed perform the analysis for soluble reactive phosphorus (see appendix I).

The standards for this analysis are the same as those for soluble reactive phosphorus (see appendix I).

The persulfate oxidation reagent should be used immediately and any excess should be discarded. To make the persulfate oxidation reagent dissolve 5g of potassium persulfate into 100 ml of Millipore water. To dissolve, use a stirring hotplate to heat the solution to tepid.

The reagents used to correct for pH are made as follows: Phenolphthalein indicator is made by dissolving 0.05 g phenolphthalein into a mixture of 50 ml of ethanol and 50 ml of Milipore water. The 6N NaOH is made by dissolving 120 g of NaOH in 500 ml of Milipore water. 10% HCl is made by slowly pouring 50 ml of concentrated HCl in about 300 ml of Milipore water, and then bringing the volume to 500 ml using Milipore water.

Appendix C

Nitrite Analysis

Triplicate 5 ml aliquots of each sample and Milipore water, as well as, duplicate 5 ml aliquots of 5 µmol/liter, 10 µmol/liter, and 20 µmol/liter standards are put into acid-rinsed centrifuge tubes. 1 ml of Strickland buffer is added to each tube followed by 250 µl of sulfanilamide solution. After the sulfanilamide solution is added, the tube should be swirled using a vortexer. Exactly six minutes after the addition of the sulfanilamide solution, 250 µl of naphthylethylene solution should be added and the tubes once again swirled using a vortexer. The absorbance can be measured after ten minutes using a spectrophotometer set at a wavelength of 540 or 543 nm using a 1 cm cuvette. The absorbance should be measured before two hours' time.

The standards for this analysis were made using a standard solution of 0.3450 g Sodium Nitrite dissolved into 1000 ml of Milipore water. Using the standard solution 1 ml was added to 1000 ml, 500 ml, and 250 ml to create standards of 5 µmol/liter, 10 µmol/liter, and 20 µmol/liter of phosphate. The standard solution and standards should be made on the day of analysis.

To make the Strickland buffer dissolve 75 g of ammonium chloride in 400 ml of Milipore water. After the ammonium chloride is dissolved adjust the pH to 8.5 by adding NH_4OH while monitoring pH using a pH meter. Once pH is at 8.5, bring the volume to 500 ml using Milipore water. The Strickland buffer can be stored for many months.

The sulfanilamide solution is made by dissolving 5 g of sulfanilamide in a solution of 50 ml concentrated HCl and 300 ml of Milipore water. Once all sulfanilamide is dissolved bring volume to 500 ml using Milipore water. The sulfanilamide solution can be stored for many months.

The naphthylethylene solution is made by dissolving 0.5 g N-(1-naphthyl) ethylene diamine dihydrochloride in 500 ml of Milipore water. The naphthylethylene

solution should be stored in an amber bottle and renewed monthly or when solution turns brown.

Appendix D

Nitrate Analysis

Acid rinsed centrifuge tubes are preloaded with 0.25-0.30 g of spongy cadmium and 1 ml of Strickland buffer. Then triplicate 5 ml aliquots of each sample and Milipore water, as well as, duplicate 5 ml aliquots of 5 µmol/liter, 10 µmol/liter, and 20 µmol/liter standards; for both nitrite and nitrate; are put into preloaded tubes. The tubes are then organized horizontally on a shaker table and shaken at 100 excursions per minute for 2 hours. After 2 hours 250 µl of sulfanilamide solution is added and the tube should be swirled using a vortexer. Exactly six minutes after the addition of the sulfanilamide solution, 250 µl of naphthylethylene solution should be added and the tubes once again swirled using a vortexer. The absorbance can be measured after ten minutes using a spectrophotometer set at a wavelength of 540 or 543 nm using a 1 cm cuvette. The absorbance should be measured before two hours' time.

The nitrate standards for this analysis where made using a standard solution of 0.4250 g sodium nitrate dissolved into 1000 ml of Milipore water. Using the standard solution, 1 ml was added to 1000 ml, 500 ml, and 250 ml to create standards of 5 µmol/liter, 10 µmol/liter, and 20 µmol/liter of phosphate. The standard solution can be refrigerated and stored for months, but the standards should be made on the day of analysis. For instructions on making the nitrite standards see Appendix III.

To prepare the spongy cadmium first make the cadmium sulfate solution by dissolving 20 g of cadmium sulfate in 100 ml of Milipore water. To clean both the spongy cadmium and the zinc strips used in this reaction, 6 N HCl should also be made by adding 492 ml of concentrated HCl to 400 ml of Milipore water, and then adjusting the volume to 1000 ml with Milipore water. After placing a zinc strip in a graduated cylinder cadmium sulfate solution until the zinc strip is cover by approximately 20 ml, and let sit overnight. The spongy cadmium will precipitate out onto the zinc strip. The next day

remove the zinc strip and; using a plastic spatula; scrape the precipitate into a beaker. After removing as much precipitate as possible clean the zinc with 6 N HCl, rinse many times with Milipore water, and then allow to thoroughly dry before storing for later use. Drain any remaining cadmium sulfate from the spongy cadmium precipitate, break the spongy cadmium into small granules, then acidify them with 6 N HCl ;for no more than a few minutes; and then rinse twenty times with Milipore water. After using the spongy cadmium for nitrate analysis the cadmium can be regenerated by repeating the acidification steps until complete dissolution of the spongy cadmium occurs. Spongy cadmium can be stored in a covered beaker with Milipore water. Instruction for making the Strickland buffer, sulfanilamide solution, and naphthylethylene solution can be found in Appendix III.

Appendix E

Ammonium Analysis

Triplicate 25 ml aliquots of each sample and Milipore water, as well as, duplicate 25 ml aliquots of 5 µmol/liter, 10 µmol/liter, and 20 µmol/liter standards are put into dedicated Wheaton bottles. 1 ml of phenol solution, 1 ml of nitroferricyanide, and 2.5 ml of oxidizing solution is added to each Wheaton bottle. The caps are then replaced and the bottles are let to stand for one hour. The absorbance of each bottle can then be measured using a spectrophotometer set at wavelength 640 nm using a 1 cm cuvette.

The wheaton bottles used for this analysis should not be used for any other nutrient analysis because it will cause interference. After each use the excess sample should be discarded and approximately 50 ml of Milipore water should be placed in the bottle to remain will stored. The bottles should be rinsed several times before use.

The standards for this analysis where made using a standard solution of 0.3303 g of ammonium sulfate dissolved into 1000 ml of Milipore water to form 5 mmol/liter solution. Using the standard solution 1 ml was added to 1000 ml, 500 ml, and 250 ml to create standards of 5 µmol/liter, 10 µmol/liter, and 20 µmol/liter of phosphate. The standard solution can be refrigerated and stored for months, but the standards should be made on the day of analysis

To make the phenol solution, dissolve 20 g of phenol into 200 ml of 95% ethanol. The phenol solution must be stored in an amber container and kept refrigerated. The solution should be stable for at least on month.

To make nitroferricyanide, dissolve 1.0 g sodium nitroferricyanide into 200 ml of Milipore water. The nitroferricyanide solution must be stored in an amber container and kept refrigerated. The solution should be stable for at least on month.

The oxidizing solution is made by mixing 100 ml of citric acid solution and 25 ml of commercial hydrochlorite. The citric acid solution is made by dissolving 100 g of citric acid and 5 g of sodium hydroxide in 500 ml of Milipore water. The citric acid solution can

be stored indefinitely, but the oxidizing solution should be made on the day of the analysis and kept stoppered.

Appendix F

Soluble Reactive Silicate

Triplicate 25 ml aliquots of each sample and Milipore water, as well as, duplicate 25 ml aliquots of 10 µmol/liter, 20 µmol/liter, and 50 µmol/liter standards are put into plastic tri-pour beakers due to interference caused by silica dissolution in glass containers. 10 ml of molybdate reagent, then after ten minutes 15 ml of the reducing reagent is added. Aluminum foil is placed over the beakers to prevent contamination by dust. The absorbance of each bottle can then be measured using a spectrophotometer set at wavelength 810 nm after 2-3 hours using a 1cm cuvette.

The standards for this analysis where made using a standard solution of 2.8420 g Sodium metasilicate nonahydrate dissolved into 1000 ml of Milipore water. Using the standard solution 1 ml was added to 500 ml, 250 ml, and 100 ml to create standards of 10 µmol/liter, 20 µmol/liter, and 50 µmol/liter of phosphate. The standard solution can be refrigerated and stored for months, but the standards should be made on the day of analysis.

The molybdate reagent is made by dissolving 4.0 g of ammonium molybdate in approximately 300 ml of Milipore water, then adding 12 ml of concentrated HCL, and then bringing the volume to 500 ml with Milipore water. Store the molybdate reagent in a polyethylene container. The molybdate reagent should be stable for many months, but if a white precipitate forms discard.

To make the reducing reagent is a mixture of 80 ml of Milipore water and three solutions; 100 ml of the metol-sulfite solution, 60 ml of the oxalic acid solution, and 60 ml of the sulfuric acid solution. The metol-sulfite solution is made by dissolving 6 g of anhydrous sodium sulfite in 500 ml of Milipore water, then adding 10 g of metol (p-methylaminophenol sulfate), and storing in a tightly stoppered glass bottle to be remade monthly. The oxalic acid solution is made by dissolving 50 g of oxalic acid dehydrate into 500 ml of Milipore water and stored for many months. The sulfuric acid solution is made

by adding 250 ml of concentrated sulfuric acid into 250 ml Milipore water, cooling to room temperature, and then bringing the volume back to 500 ml using Milipore water.

Appendix G

Correlations between Secchi disk depth and macro-nutrients to precipitation

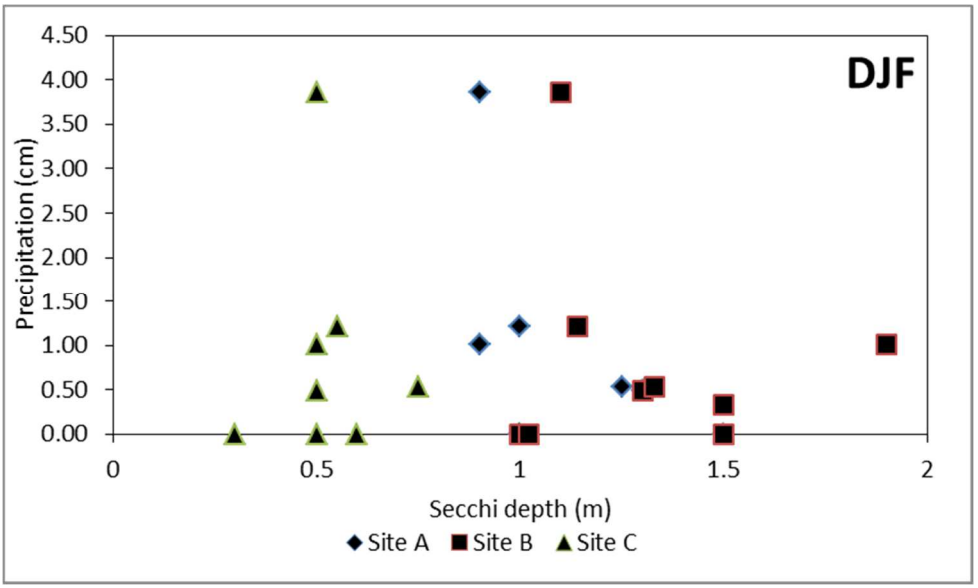

Figure G.1 Correlation between precipitation and Secchi disk depth during the period from December through January of this study.

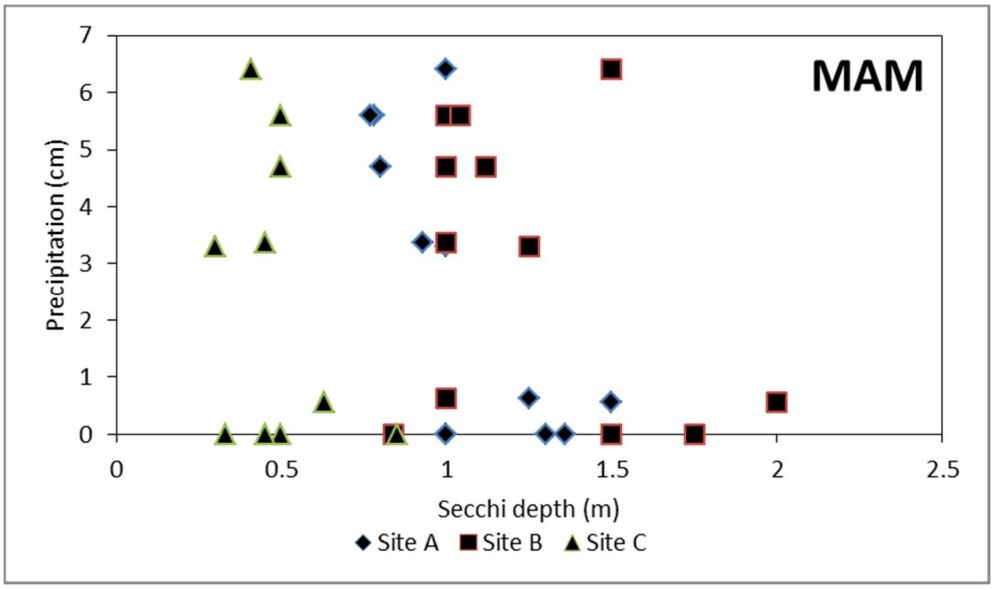

Figure G.2 Correlation between precipitation and Secchi disk depth during the period from March through May of this study.

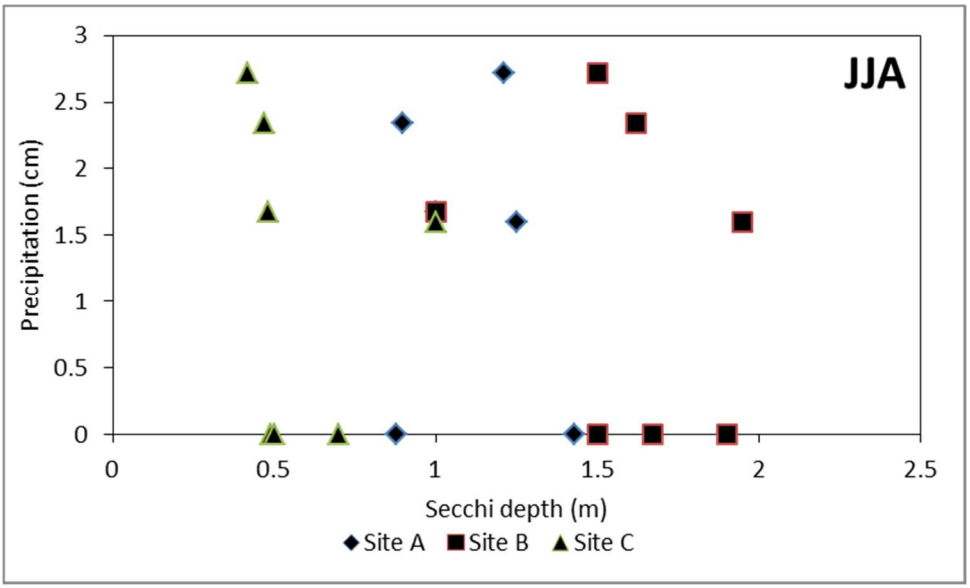

Figure G.3 Correlation between precipitation and Secchi disk depth during the period from June through August of this study.

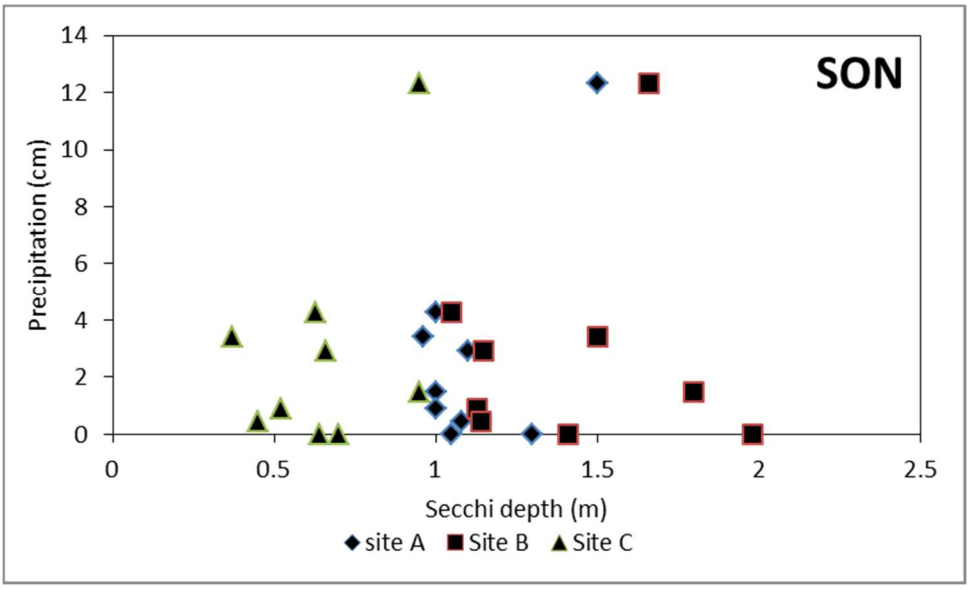

Figure G.4 Correlation between precipitation and Secchi disk depth during the period from September through November of this study.

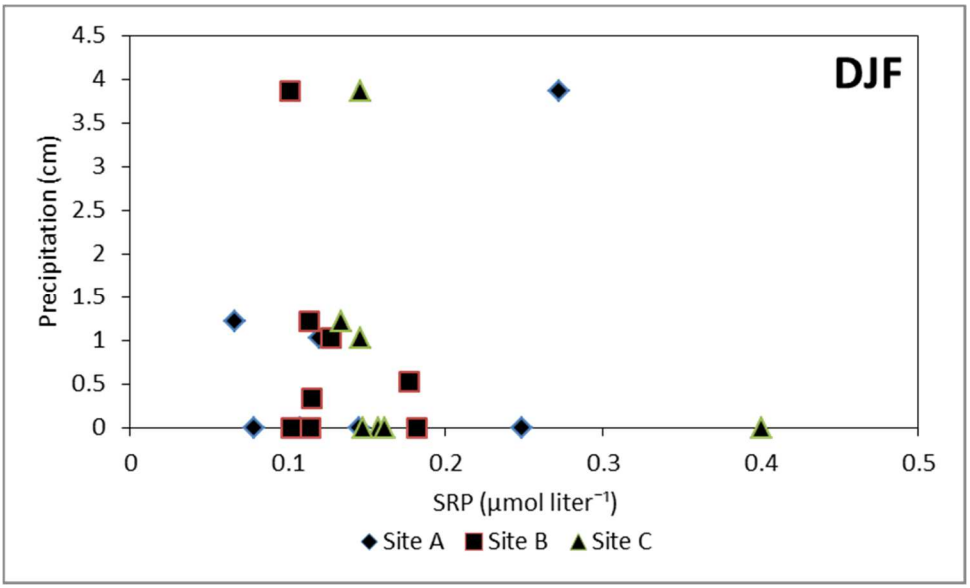

Figure G.5 Correlation between precipitation and SRP during the period from December through January of this study.

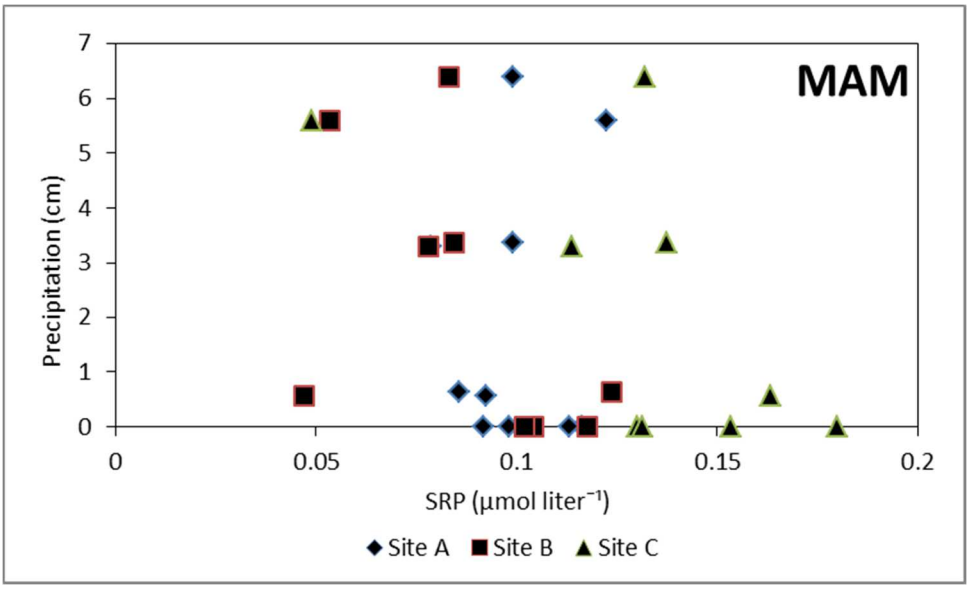

Figure G.6 Correlation between precipitation and SRP during the period from March through May of this study.

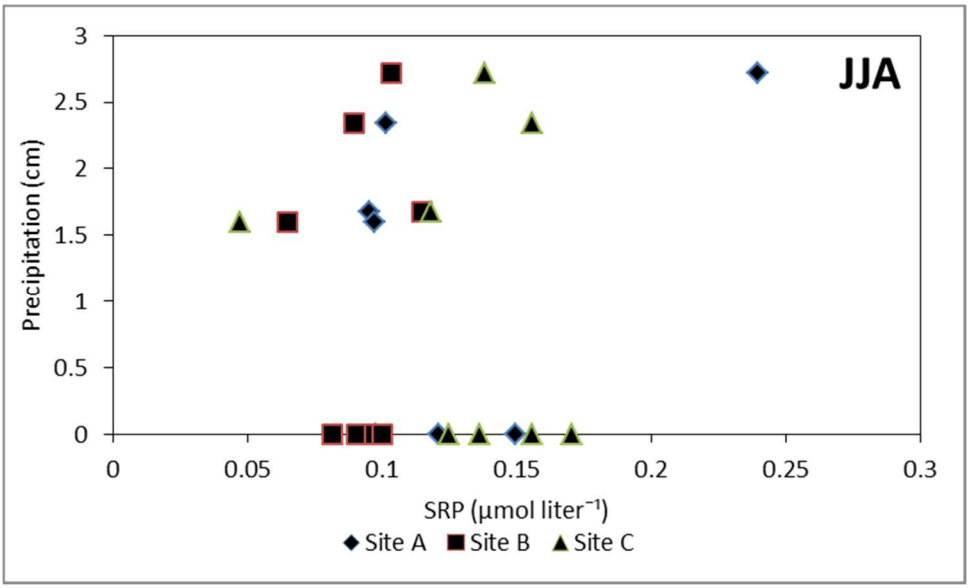

Figure G.7 Correlation between precipitation and SRP during the period from June through August of this study.

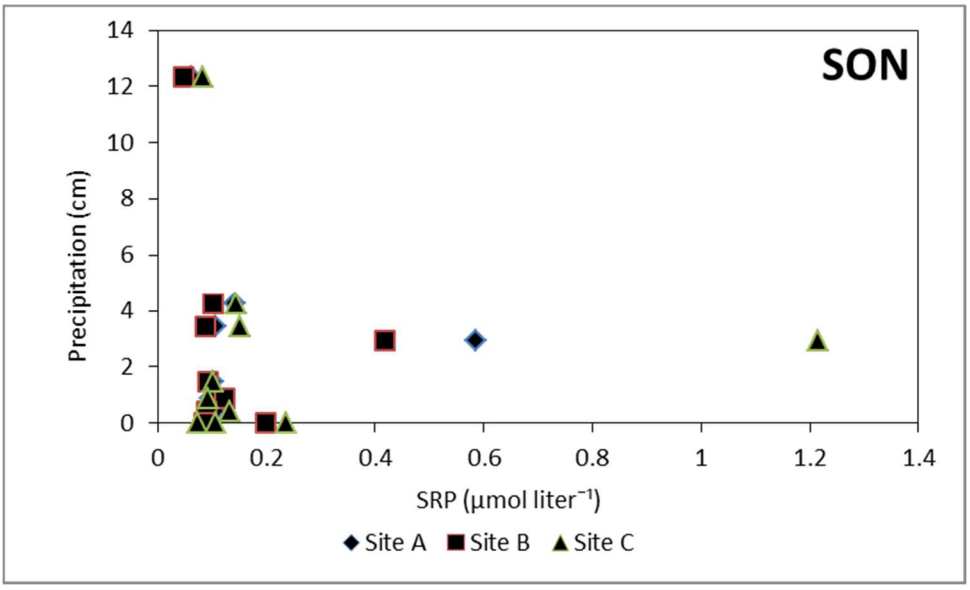

Figure G.8 Correlation between precipitation and SRP during the period from September through November of this study.

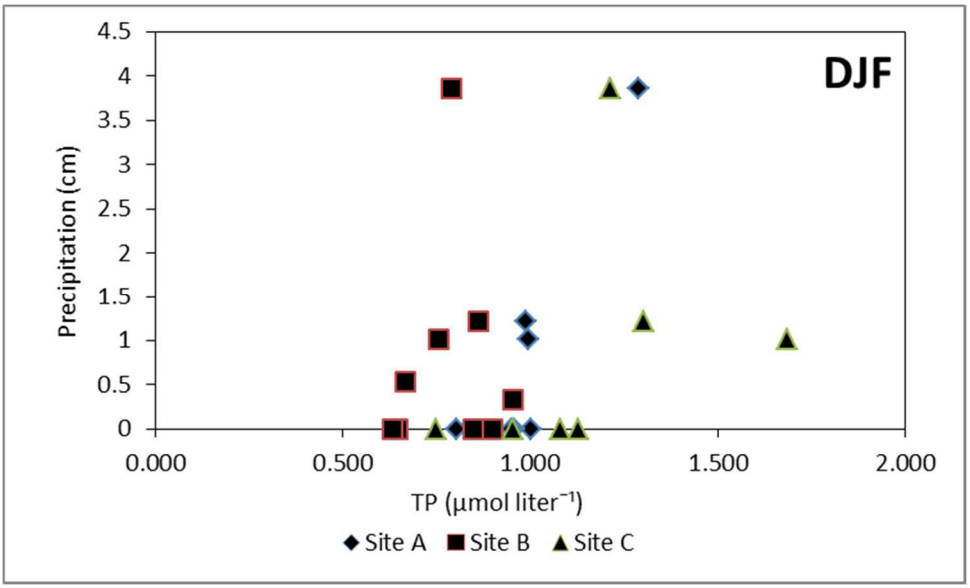

Figure G.9 Correlation between precipitation and TP during the period from December through January of this study.

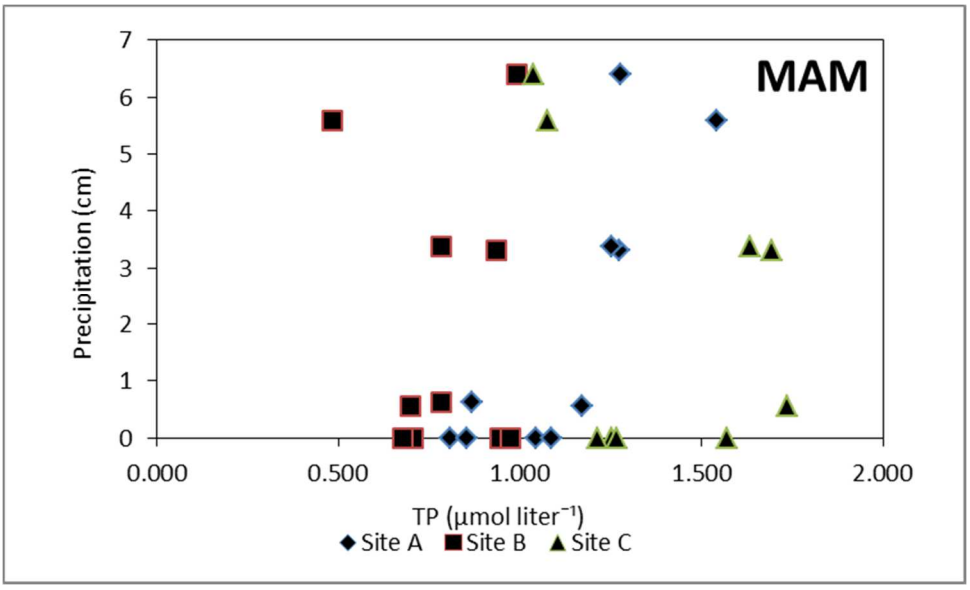

Figure G.10 Correlation between precipitation and TP during the period from March through May of this study.

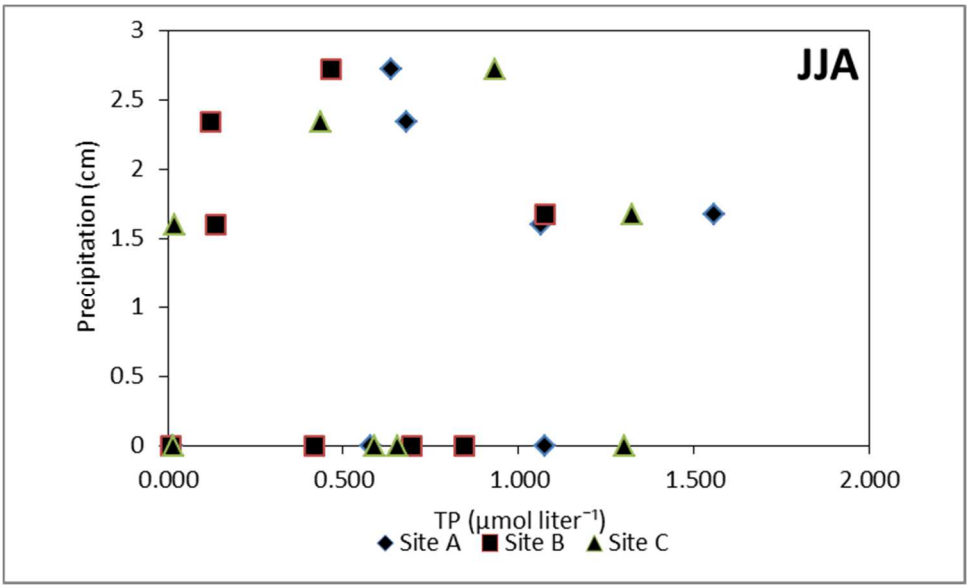

Figure G.11 Correlation between precipitation and TP during the period from June through August of this study.

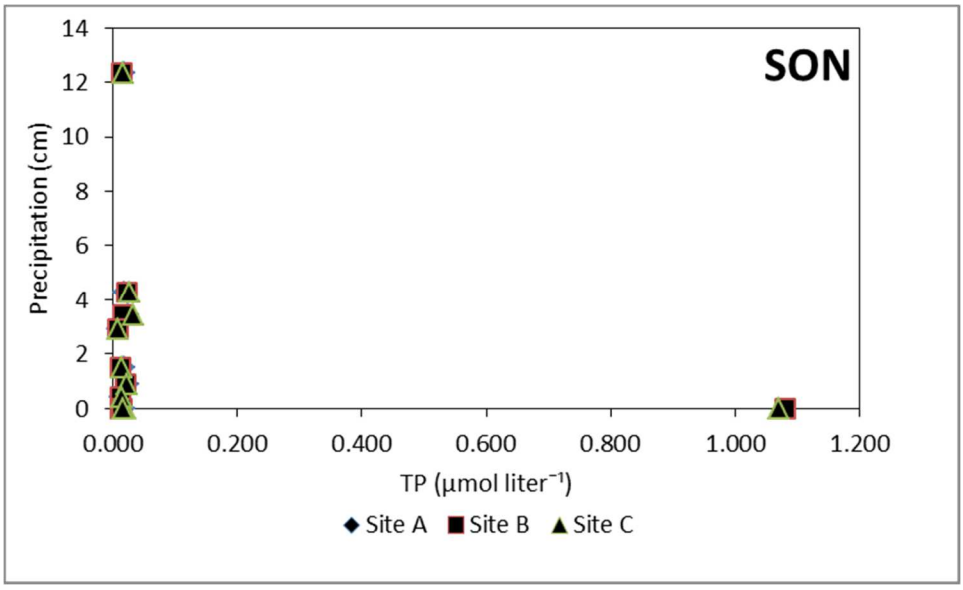

Figure G.12 Correlation between precipitation and TP during the period from September through November of this study.

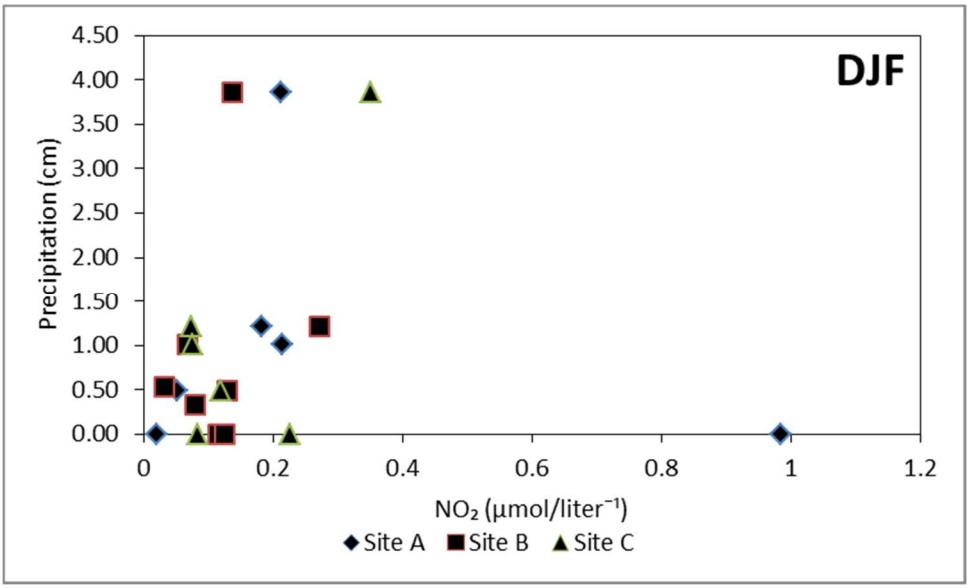

Figure G.13 Correlation plot depicting the correlation between precipitation and NO_2 disk depth during the period from December through January of this study.

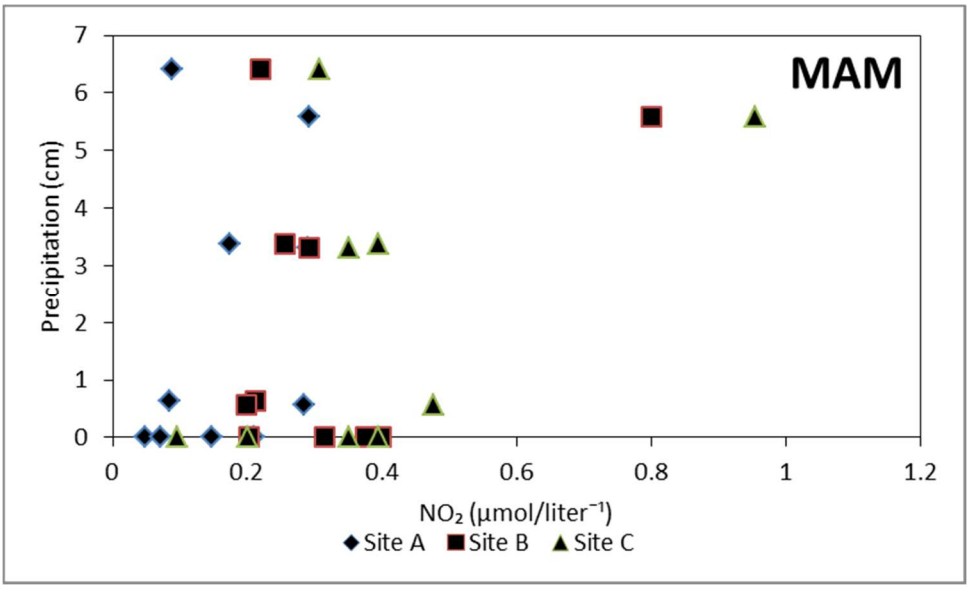

Figure G.14 Correlation between precipitation and NO_2 during the period from March through May of this study.

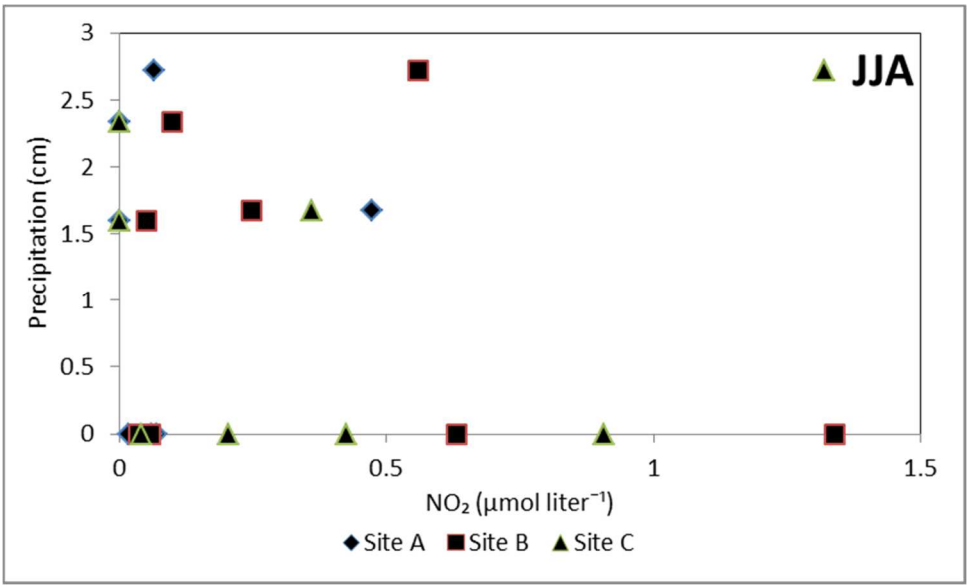

Figure G.15 Correlation between precipitation and NO_2 during the period from June through August of this study.

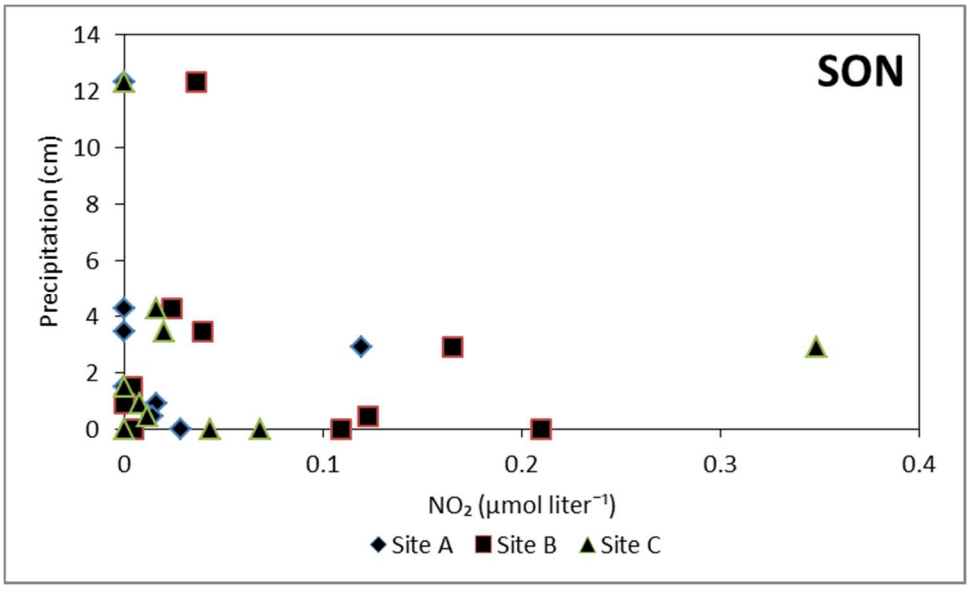

Figure G.16 Correlation plot depicting the correlation between precipitation and NO_2 during the period from September through November of this study.

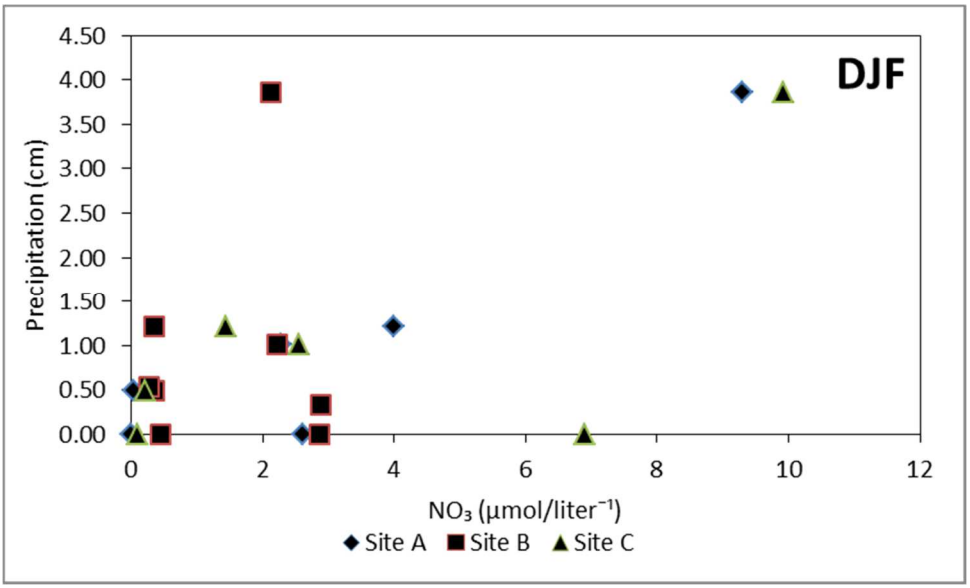

Figure G.17 Correlation plot depicting the correlation between precipitation and NO_3 during the period from December through February of this study.

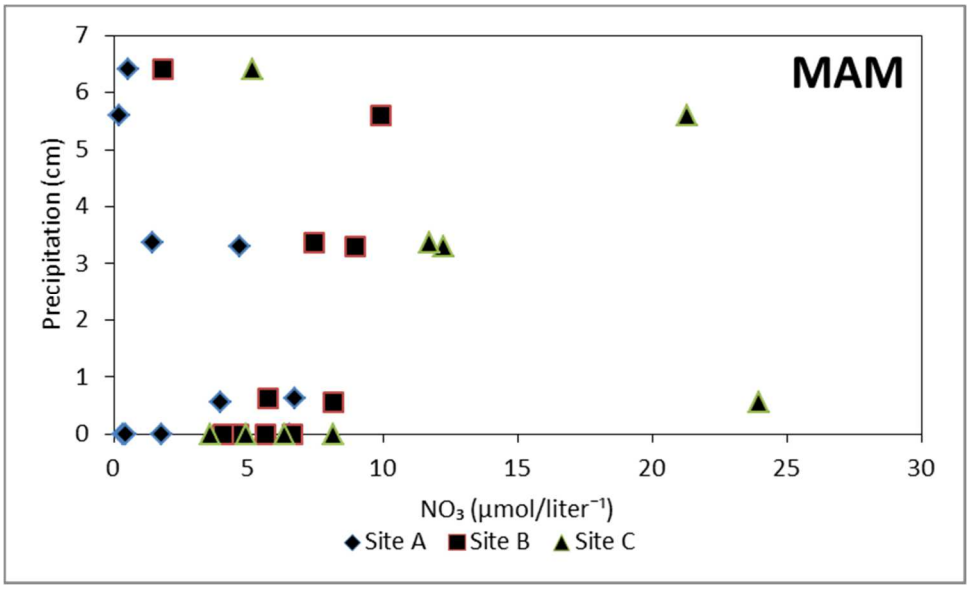

Figure G.18 Correlation between precipitation and NO_3 during the period from March through May of this study.

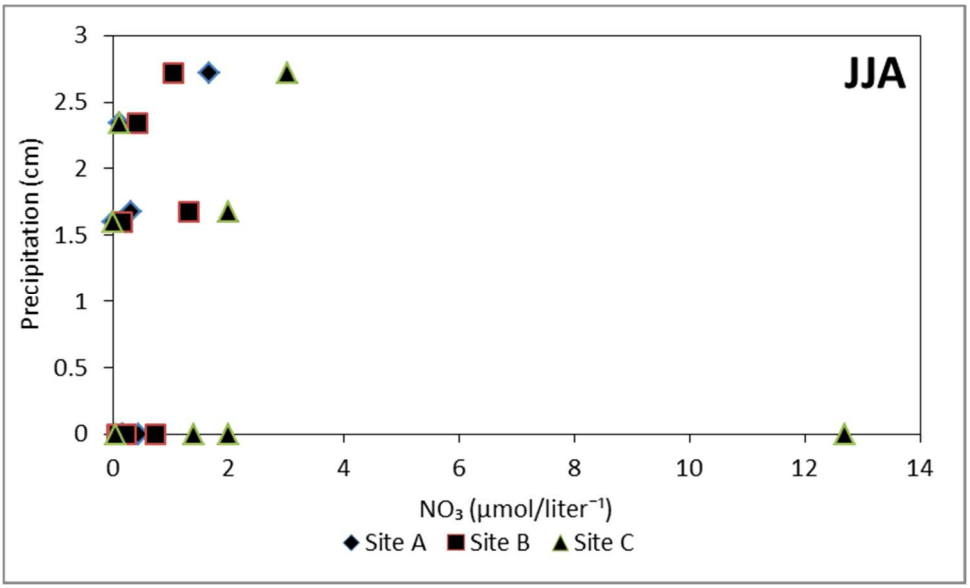

Figure G.19 Correlation between precipitation and NO_3 during the period from June through August of this study.

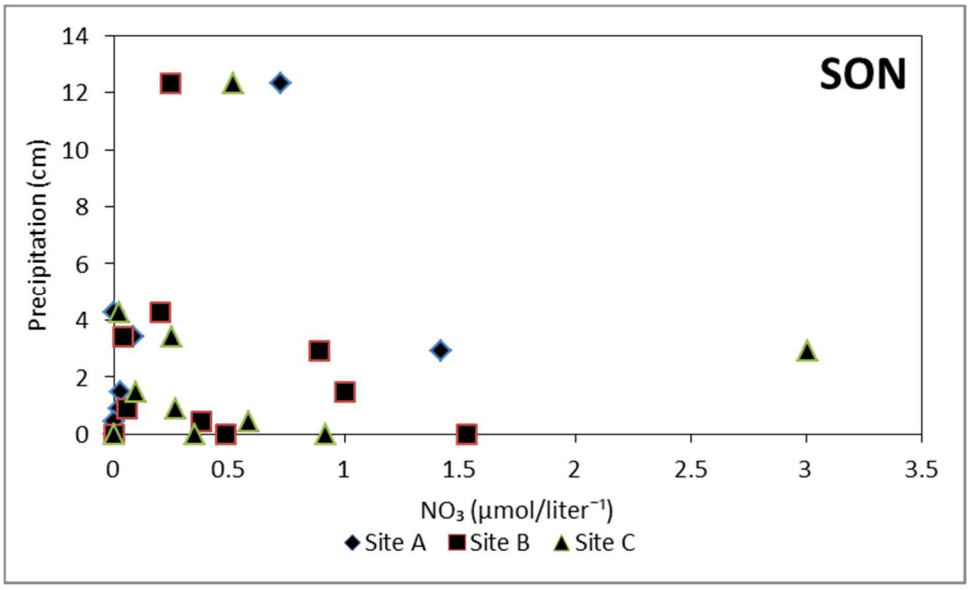

Figure G.20 Correlation between precipitation and NO_3 during the period from September through November of this study.

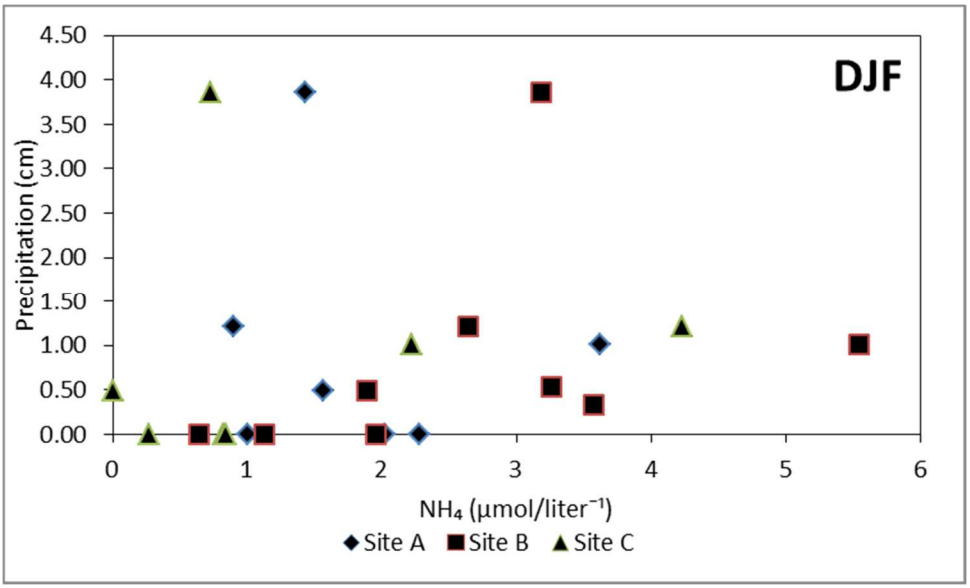

Figure G.21 Correlation between precipitation and NH_4 during the period from December through February of this study.

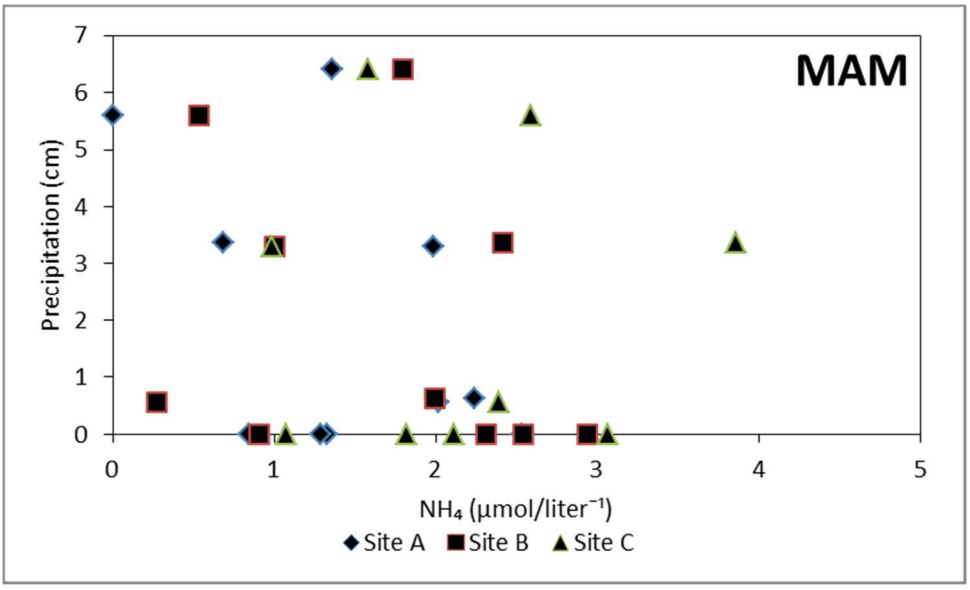

Figure G.22 Correlation between precipitation and NH_4 during the period from March through May of this study.

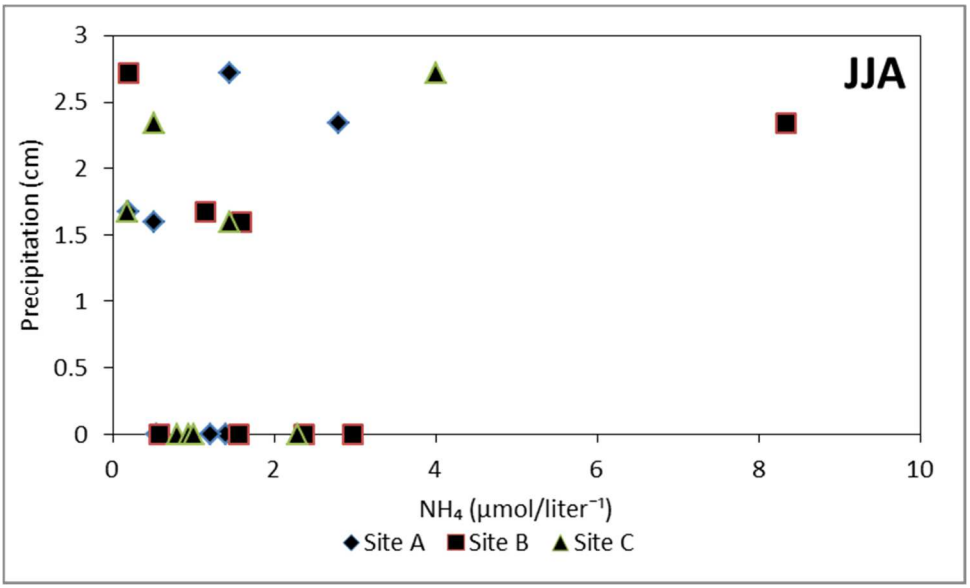

Figure G.23 Correlation between precipitation and NH_4 during the period from June through August of this study.

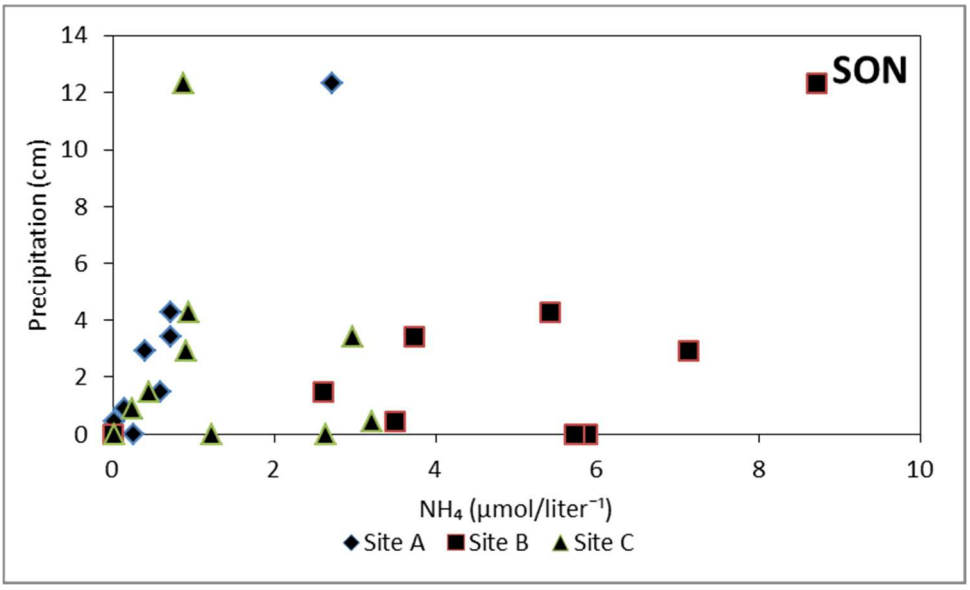

Figure G.24 Correlation between precipitation and NH_4 during the period from September through November of this study.

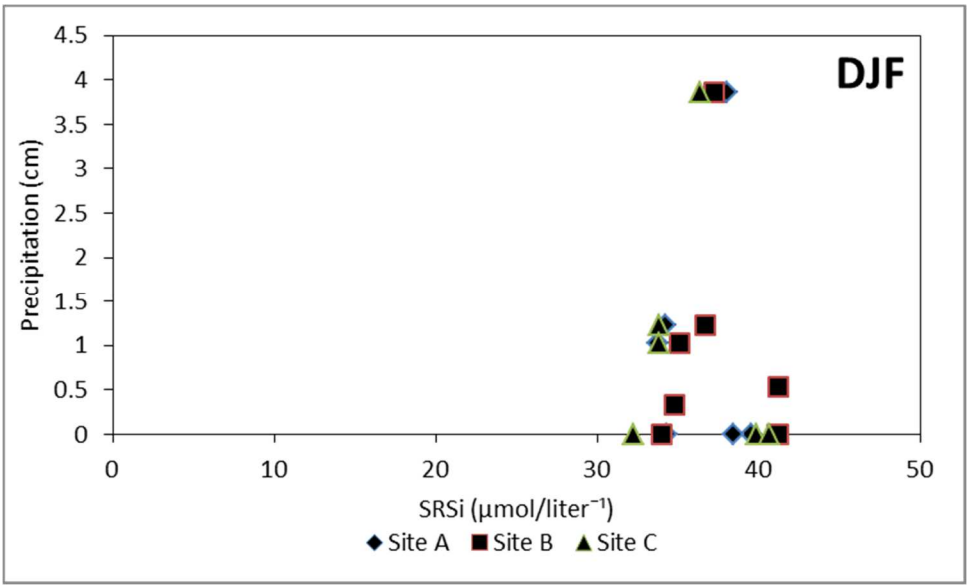

Figure G.25 Correlation between precipitation and SRSi during the period from December through January of this study.

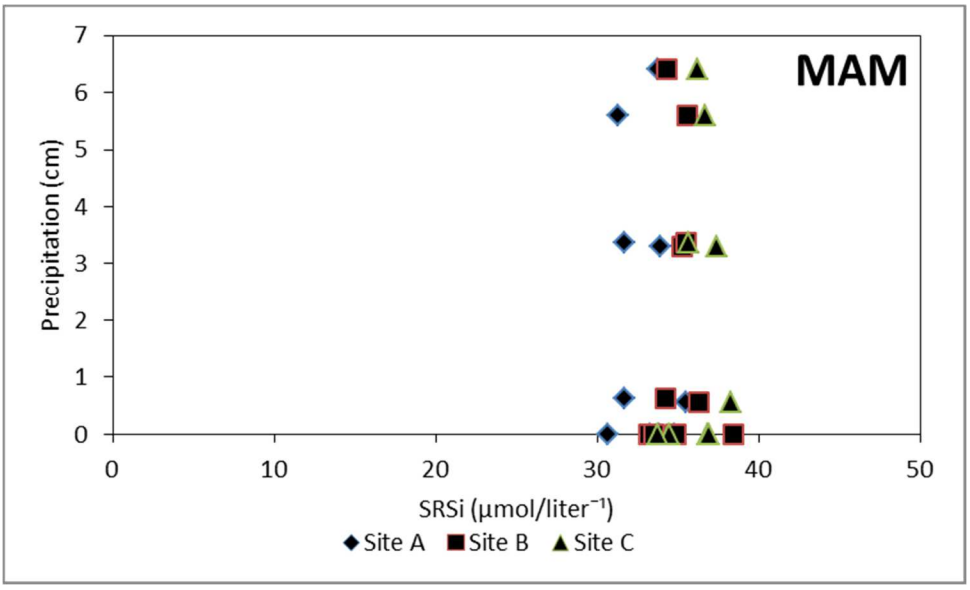

Figure G.26 Correlation between precipitation and SRSi during the period from March through May of this study.

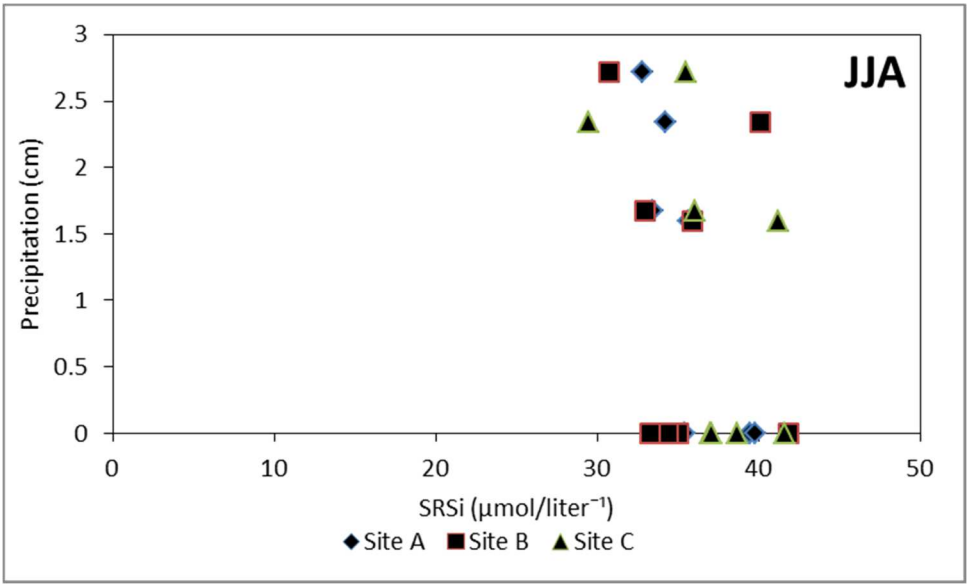

Figure G.27 Correlation between precipitation and SRSi during the period from June through August of this study.

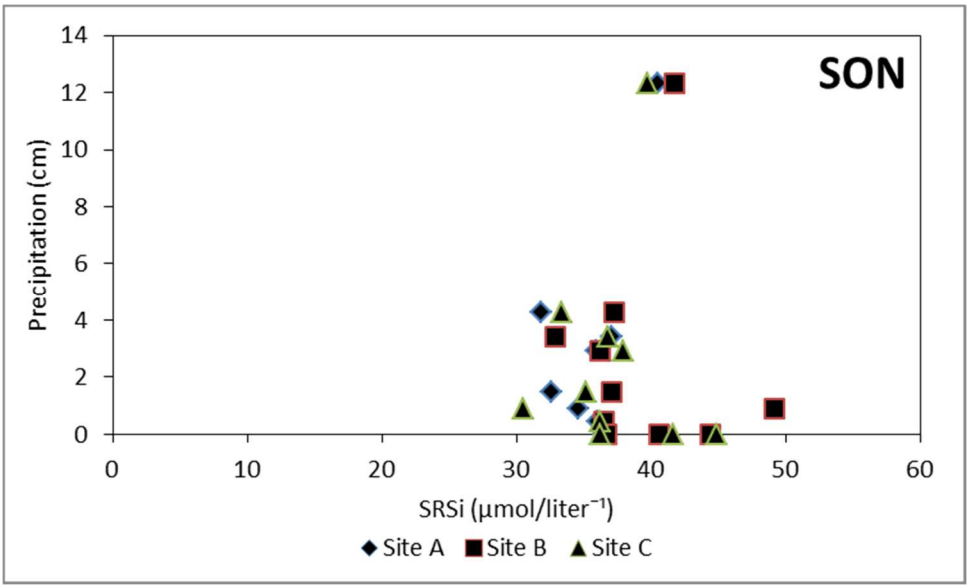

Figure G.28 Correlation between precipitation and SRSi during the period from September through November of this study.

Appendix H

Density calculation

Table H.1 Table indicating water density (kg/m^3) at temperature (°C) (UNESCO 1981).

Temp. (°C)	Density (kg/m^3)	Temp. (°C)	Density (kg/m^3)	Temp. (°C)	Density (kg/m^3)	Temp. (°C)	Density (kg/m^3)	Temp. (°C)	Density (kg/m^3)
0.0	999.84	3.5	999.97	7.0	999.90	10.5	999.66	14.0	999.25
0.1	999.85	3.6	999.97	7.1	999.90	10.6	999.65	14.1	999.23
0.2	999.86	3.7	999.97	7.2	999.89	10.7	999.64	14.2	999.22
0.3	999.86	3.8	999.97	7.3	999.89	10.8	999.63	14.3	999.20
0.4	999.87	3.9	999.97	7.4	999.88	10.9	999.62	14.4	999.19
0.5	999.87	4.0	999.98	7.5	999.88	11.0	999.61	14.5	999.18
0.6	999.88	4.1	999.97	7.6	999.87	11.1	999.60	14.6	999.16
0.7	999.89	4.2	999.97	7.7	999.87	11.2	999.59	14.7	999.15
0.8	999.89	4.3	999.97	7.8	999.86	11.3	999.58	14.8	999.13
0.9	999.90	4.4	999.97	7.9	999.86	11.4	999.57	14.9	999.12
1.0	999.90	4.5	999.97	8.0	999.85	11.5	999.56	15.0	999.10
1.1	999.91	4.6	999.97	8.1	999.84	11.6	999.54	15.1	999.09
1.2	999.91	4.7	999.97	8.2	999.84	11.7	999.53	15.2	999.07
1.3	999.92	4.8	999.97	8.3	999.83	11.8	999.52	15.3	999.06
1.4	999.92	4.9	999.97	8.4	999.83	11.9	999.51	15.4	999.04
1.5	999.92	5.0	999.97	8.5	999.82	12.0	999.50	15.5	999.02
1.6	999.93	5.1	999.97	8.6	999.81	12.1	999.49	15.6	999.01
1.7	999.93	5.2	999.96	8.7	999.81	12.2	999.48	15.7	998.99
1.8	999.94	5.3	999.96	8.8	999.80	12.3	999.46	15.8	998.98
1.9	999.94	5.4	999.96	8.9	999.79	12.4	999.45	15.9	998.96
2.0	999.94	5.5	999.96	9.0	999.78	12.5	999.44	16.0	998.94
2.1	999.95	5.6	999.95	9.1	999.78	12.6	999.43	16.1	998.93
2.2	999.95	5.7	999.95	9.2	999.77	12.7	999.42	16.2	998.91
2.3	999.95	5.8	999.95	9.3	999.76	12.8	999.40	16.3	998.90
2.4	999.95	5.9	999.95	9.4	999.75	12.9	999.39	16.4	998.88
2.5	999.96	6.0	999.94	9.5	999.74	13.0	999.38	16.5	998.86
2.6	999.96	6.1	999.94	9.6	999.74	13.1	999.37	16.6	998.85
2.7	999.96	6.2	999.94	9.7	999.73	13.2	999.35	16.7	998.83
2.8	999.96	6.3	999.93	9.8	999.72	13.3	999.34	16.8	998.81
2.9	999.97	6.4	999.93	9.9	999.71	13.4	999.33	16.9	998.79
3.0	999.97	6.5	999.93	10.0	999.70	13.5	999.31	17.0	998.78
3.1	999.97	6.6	999.92	10.1	999.69	13.6	999.30	17.1	998.76
3.2	999.97	6.7	999.92	10.2	999.68	13.7	999.29	17.2	998.74
3.3	999.97	6.8	999.91	10.3	999.68	13.8	999.27	17.3	998.72
3.4	999.97	6.9	999.91	10.4	999.67	13.9	999.26	17.4	998.71

Table H.1 - *Continued*

17.5	998.69	20.2	998.16	22.9	997.56	25.6	996.89	28.3	996.15
17.6	998.67	20.3	998.14	23.0	997.54	25.7	996.87	28.4	996.12
17.7	998.65	20.4	998.12	23.1	997.52	25.8	996.84	28.5	996.09
17.8	998.63	20.5	998.10	23.2	997.49	25.9	996.81	28.6	996.07
17.9	998.62	20.6	998.08	23.3	997.47	26.0	996.79	28.7	996.04
18.0	998.60	20.7	998.06	23.4	997.45	26.1	996.76	28.8	996.01
18.1	998.58	20.8	998.04	23.5	997.42	26.2	996.73	28.9	995.98
18.2	998.56	20.9	998.02	23.6	997.40	26.3	996.71	29.0	995.95
18.3	998.54	21.0	997.99	23.7	997.37	26.4	996.68	29.1	995.92
18.4	998.52	21.1	997.97	23.8	997.35	26.5	996.65	29.2	995.89
18.5	998.50	21.2	997.95	23.9	997.32	26.6	996.63	29.3	995.86
18.6	998.48	21.3	997.93	24.0	997.30	26.7	996.60	29.4	995.83
18.7	998.47	21.4	997.91	24.1	997.27	26.8	996.57	29.5	995.80
18.8	998.45	21.5	997.89	24.2	997.25	26.9	996.54	29.6	995.77
18.9	998.43	21.6	997.86	24.3	997.23	27.0	996.52	29.7	995.74
19.0	998.41	21.7	997.84	24.4	997.20	27.1	996.49	29.8	995.71
19.1	998.39	21.8	997.82	24.5	997.17	27.2	996.46	29.9	995.68
19.2	998.37	21.9	997.80	24.6	997.15	27.3	996.43	30.0	995.65
19.3	998.35	22.0	997.77	24.7	997.12	27.4	996.41	30.1	995.62
19.4	998.33	22.1	997.75	24.8	997.10	27.5	996.38	30.2	995.59
19.5	998.31	22.2	997.73	24.9	997.07	27.6	996.35	30.3	995.56
19.6	998.29	22.3	997.70	25.0	997.05	27.7	996.32	30.4	995.53
19.7	998.27	22.4	997.68	25.1	997.02	27.8	996.29	30.5	995.50
19.8	998.25	22.5	997.66	25.2	997.00	27.9	996.27	30.6	995.47
19.9	998.23	22.6	997.64	25.3	996.97	28.0	996.24	30.7	995.44
20.0	998.21	22.7	997.61	25.4	996.94	28.1	996.21	30.8	995.41
20.1	998.19	22.8	997.59	25.5	996.92	28.2	996.18	30.9	995.38

References

Army Corp of Engineers, 1999. Welcome to Joe Pool Lake, [Online available www.swf-wc.usace.army.mil/joepool/.]

Bjerknes, J., 1969. Atmospheric teleconnections from the equatorial pacific. Journal of Physical Oceanography. 97(3): 163-172.

Bjerknes, J., 1964. Atlantic air–sea interaction. Advances in Geophysics. Academic Press. 10: 1-82.

Blenckner, T. 2005. A conceptual model of climate-related effects on lake ecosystems. Hydrobiolgia. 533: 1-13.

Boehrer, B., and M. Schultze, 2008. Stratification of lakes. Reviews of Geophysics. 46: 1-27.

Carey, R.O., 2013. Evaluating nutrient impacts in urban watersheds: challenges and research opportunities. Environmental Pollution. 173: 138-149.

Celik, K., and J. Schindler, 2006. The vertical distribution of phytoplankton assemblages of Lake James, North Carolina in relation to mixing depth and nitrate and phosphate concentrations. Ohio J. Sci. 4: 136-145.

Chrzanowski, T.H., and J.P. Grover, 2001. Effects of mineral nutrients on the growth of bacterio- and phytoplankton in two southern reservoirs. *Limnol. Oceanogr.* 46: 1319-1330.

Chrzanowski, T.H., and J.P. Grover, 2005. Temporal coherence in limnological features of two southeastern reservoirs. *Lake and Reservoir Management* 21: 39-48.

D'Aleo, J., and D. Easterbrook, 2010. Multidecadal tendencies in ENSO and global temperatures related to multidecadal oscillations. Energy and Environment. 21 (5): 437-460.

De Stasio Jr., B.T., D.K. Hill, J.M. Kleinhans, N.P. Nibbelink, and J.J. Magnuson, 1996. Potential effects of global climate change on small north-temperate lakes: Physics, fish, and plankton. Limnol. Oceanogr. 41: 1136–1149.

Ellis, H. T., and R.F. Pueschel, 1971. Solar radiation: absence of air pollution trends at Mauna Loa. Science. 172: 845-846.

England, M.H., S. McGregor, P. Spence, G.A. Meehl, A. Timmermann, W. Cai, A.S. Gupta, M.J. McPhaden, A. Purich, and A. Santoso, 2014. Recent intensification of wind-driven circulation in the Pacific and the ongoing warming hiatus. Nature Climate Change 4: 222-227.

Feely, R. A., S. C. Doney, and S. R. Cooley, 2009. Ocean acidification: Present conditions and future changes in a high-CO2 world. Oceanography 22(4): 36–47.

Gorham,E., J.K. Underwood, F.B. Martini, and J.G. Ogden III, 1986. Natural and anthropogenic causes of lake acidification in Nova Scotia. Nature. 324: 451-453.

Grover, J.P., and T.H. Chrzanowski, 2000. Seasonal patterns substrate utilization by bacterioplankton: case studies in four temperate lakes of different latitudes. Aquatic Microbial Ecology. 23: 41-54.

Grover, J.P., and T.H. Chrzanowski, 2004. Limiting resources, disturbance, and diversity in phytoplankton communities. Ecological Monographs. 74: 533-551.

Grover, J.P., and T.H. Chrzanowski, 2005. Seasonal dynamics of phytoplankton in two warm temperate reservoirs: association of taxonomic composition with temperature. J. Plankton Res. 27: 1-17.

IPCC, 2013. Climate change 2013: the physical science basis, p. 1535. In T. F. Stocker, D. Qin, G.-K. Plattner, M. Tignor, S.K. Allen, J. Boschung, A. Nauels, Y. Xia, V. Bex and P.M. Midgley [eds], Contribution of Working Group I to the Fifth Assessment Report of the Intergovern- mental Panel on Climate Change. Cambridge University Press, Cambridge, United Kingdom and New York, NY, USA.

Hasler, A. D., 1947. Eutrophication of lakes by domestic sewage. *Ecology 2*8: 383-395.

Holling, C. S., 1973. Resilience and stability of ecological systems. Annual Review of Ecology and Systematics. 4:1-23.

Hutchinson, G.E., 1957. A Treatise on Limnology Geography, Physics, and Chemistry, Vol.1. John Wiley & Sons, New York, NY.

Hutchinson, G. E. and H. Löffler, 1956. The thermal classification of lakes. Proc. Nat. Acad. Sci. 42: 84-86.

Jeppesen, E., M., Søndergaard, N. Mazzeo, M. Meerhoff, C. Branco, V. Huszar, and F. Scasso, 2005. Lake restoration and biomanipulation in temperate lakes: relevance for subtropical and tropical lakes, p. 331-359. In M.V. Reddy [eds], Tropical eutrophic lakes: their restoration and management.

Jones, M.N., 1984. Nitrate reduction by shaking with cadmium: alternative to cadmium columns. Water Research. 18: 643-646.

Kennedy, R.H., and W.W. Walker, 1990. Reservoir nutrient dynamics. p. 109–131 In K.W.Thornton, B.L. Kimmel, F.E. Payne [eds], Reservoir Limnology: Ecological Perspectives. John Wiley & Sons, Inc., New York, NY.

Kimmel, B.L., O.T. Lind, and L.J. Paulson. 1990, In K.W. Thornton, B.L. Kimmel, F.E. Payne [eds.], Reservoir Limnology: Ecological Perspectives. John Wiley & Sons, Inc., New York, NY. p. 133–193

Kimmel, B.L., and A.W. Groeger, 1984. Factors controlling primary production in lakes and reservoirs: a perspective. p. 277–281 In Proceedings of the North American Lake Management Society. EPA 440/5/84-001. United States Environmental Protection Agency, Washington, DC.

Kirchner, I. G.L. Stenchikov, H.F. Graf, A. Robock, and J.C. Antuña, 1999. Climate model simulation of winter warming and summer cooling following the 1991 Mount Pinatubo volcanic eruption. Journal of Geophysical Research. 104: 19039-19055.

Lampert W., Sommer U., 2007. Limnoecology. 2nd ed. Oxford University Press, Oxford. 324 pp.

Lewis, W.M. Jr., 1973. The thermal regime of Lake Lanao (Philipines) and its theoretical implications for tropical lakes. Limnology and Oceanography. 18 (2): 200-2171.

Lewis, W.M. Jr., 1983. A revised classification of lakes based on mixing. J. Fish. Aquat. Sci. 40:1779-1787.

Mackenzie A., A.S. Ball, and S.R. Virdee, 2001. Instant Notes in Ecology. 2nd edition. BIOS.

Magnuson, J.J., K.E. Webster, R.A. Assel, C.J. Bower, P.J. Dillon, J.G. Eaton, H.E. Evans, E.J. Fee, R.I. Hall, L.R. Mortsch, D.W. Schindler, and F. H. Quinn, 1997. Potential effects of climate changes on aquatic systems: Laurentian great lakes and Precambrian Shield region. Hydrological Processes. 11: 825-871.

Marshall, C.T., and R.H. Peters, 1989. General patterns in the seasonal development of chlorophyll *a* for temperate lakes. Limnology Oceanography. 34 (5): 856-867.

Meerhoff, M., J.M. Clemente, F. Teixeira De Mello, C. Iglesias, A.R. Pederson, and E. Jeppeson, 2007. Can warm climate-related structure of littoral predator assemblies weaken the clear water state in shallow lakes? Global Change Biology 13: 1888-1897.

Menzel, D.W, and N. Corwin, 1965. The measurement of total phosphorus in seawater based on the liberation of organically bound fractions by persulfate oxidation. Limnol Oceanogr. 10: 280–282.

Monson, B., 1992. A primer on limnology, 2nd edition. Water Resources Center, University of Minnesota, 1500 Cleveland Avenue, St. Paul, MN 55108, USA.

Mortimer, C.H., 1952. Water movements in lakes during summer stratification; evidence from the distribution of temperature in Windermere. Phil. Trans. Ro. Soc. London 236:355-404.

Mulholland, P.J., G. R. Best, C.C. Coutant, G.M. Hornberger, J.L. Meyer, P.J. Robinson, J.R. Stenberg, R.E. Turner, F.V. Herrera, and R.G. Wetzell, 1997. Effects of climate change on freshwater ecosystems of the South-Eastern United States and the Gulf coast of Mexico. Hydrological Processes. 11: 949-970.

Naumann, E., 1919. Några synpunkter angående limnoplanktons ökologi, Med särskild hänsyn till fytoplankton. Svensk Botanisk Tidskrift. 13:51-58.

Nielsen-Gammon, J. W., cited 2012: The 2011 Texas Drought: A Briefing Packet for the Texas Legislature October 31, 2011. [On line available: http://climatexas.tamu.edu/files/2011_drought.pdf]

Climate Prediction Center, 2014. Historical El Nino/ La Nina episodes (1950-present). [Online available http://www.cpc.ncep.noaa.gov/products/analysis_monitoring/ensostuff/ensoyears.shtml.]

NOAA, 2014. AMO (Atlantic Multidecadal Oscillation) Index (1948-present). [Online available http://www.esrl.noaa.gov/psd/data/correlation/amon.sm.data.]

NOAA, 2014. Atmospheric transmission of direct solar radiation at Mauna Loa, Hawaii. [Online available http://www.esrl.noaa.gov/gmd/grad/mloapt.html.]

NOAA. 2014. Daily summaries station details. [Online available http://www.ncdc.noaa.gov/cdo-web/datasets/GHCND/stations/GHCND:USC00414597/detail.]

Nürnberg, G. K., 1996. Trophic state of clear and colored, soft- and hard- water lakes with special consideration of nutrients, anoxia, phytoplankton and fish. Lakes and Resevoirs Management 12: 432-447.

Paulson, R.W., E.B. Chase, R.S. Roberts, and D.W. Moody, 1991. National Water Summary 1988-89. United States Government Printing Office. Denver, CO. 514 p.

Preisendorfer, R.W., 1986. Secchi disk science: visual optics of natural waters. Limnology and Oceanography 31: 909- 926.

Purcel, L.T. and R. S. Weston, 1939. The Aging of Reservoir Waters [with Discussion]. American Water Works Association 31: 1775-1806.

Reynolds, C.S., 1984. The ecology of freshwater phyto plankton. Cambridge University Press. NY. 384 p.

Salinger, M. J., J. A. Renwick, and A. B. Mullan, 2001. Interdecadal pacific oscillation and south pacific climate. International Journal of Climatology. 21: 1705–1721.

Schlesinger, M.E. and N. Ramankutty, 1994. An oscillation in the global climate system of period 65–70 years. Nature. 367: 723-726.

Schindler, D.W., 1971. Carbon, nitrogen, phosphorus and the eutrophication of freshwater lakes. Journal of Phycology. American Water Works Association. 7: 321-329.

Smith, B.T., J. L. Guyer, and A. R. Dean, 2008. The climatology, convective mode, and mesoscale environment of cool season severe thunderstorms in the Ohio and Tennessee valleys, 1995-2006. *Preprints, 24th Conference on Severe Local Storms*, American Meteorological Society, Savannah, GA. CDROM 13B.7

Søballe, D.M., B.L. Kimmel, R.H. Kennedy, and R.F. Gaugus, 1992. Reservoirs. P. 421-474. In C. T. Hackney, S. M. Adams, and W. H. Martin [eds.], Biodiversity of the southeastern United States: aquatic communities. Wiley, New York.

Solorzano, L., 1969. Determination of Ammonia in natural waters by phenolhypochlirite method. Limnology and Oceanography. 14: 799-801.

Sommer, U., Gliwicz, Z.M., Lampert, W., and Duncan, A., 1986. The PEG model of seasonal succession of planktonic events in fresh waters. Arch. Hydrobiol. 106: 433-471.

Stefan H. G., 1989. Formulation of water quality models for streams, lakes, and reservoirs: modeler's perspective. Army Corp of Engineers. E-89-1.

Stenchikov, G. L., I. Kirchner, A. Robock, H. F. Graf, J. C. Antuña, R. G. Grainger, A. Lambert, and L. W. Thomason, 1998. Radiative forcing from the 1991 Mount Pinatubo volcanic eruption. J. Geophys. Res. 103: 13,837– 13,857.

Sterner, R.W., 1994. Seasonal and spatial patterns in macro- and micro-nutrient limitation in Joe Pool Lake, Texas. Limnol. Oceanogr. 39: 535-550.

Strickland, J. S. and T.R. Parsons, 1972. A practical handbook of seawater analysis. Alger Press Ltd 2ed. pp: 1-130.

Taranu Z.E., D. Köster, R.L. Hall, T. Charette, F. Forrest, L.C. Cwyner, and I. Gregory-Eaves. 2010. Contrasting responses of dimictic and polymictic lakes to environmental change: a spatial and temporal study. Aquat. Sci. 72:97-115.

Thorton J., A. Steel, and W. Rast, 1996. Water Quality Assessments - A Guide to Use of Biota, Sediments and Water in Environmental Monitoring. 2nd ed. University Press, Cambridge. Chp 8.

UNESCO, 1981. The Practical Salinity Scale 1978 and the International Equation of State of Seawater 1980. UNESCO Technical Papers in Marine Science 36, 25 pp.

Vitousek. J. D. Aber, R. W. Howarth, G. E. Likens, P. A. Matson, D. W. Schindler, W. H. Schlesinger, and D. G. Tilman, 1997. Human alteration of the global nitrogen cycle: sources and consequences. Ecological Applications. 7: 737-750.

Volk, T. and M. I. Hoffert, 1985. Ocean carbon pumps: Analysis of relative strengths and efficiencies in ocean-driven atmospheric CO2 changes. Geophysical Monograph Series 32: 99-110.

Walker, J.L., T. Younos, and C. E Zipper, 2007. Nutrients in lakes and reservoirs- a literature review for use in nutrient criteria development. Virginia Water Resource Research Center SR34. 2007.

Weiss, R.F., 1970. The solubility of nitrogen, oxygen and argon in water and seawater. Deep-Sea Research. 17: 721-735.

Wetzel, R.G. and G.E. Likens, 1991. Limnological analysis, 2nd ed. Springer- Verlag, New York, USA.

Winguth, A.M.E, and B. Kelp., 2013. The urban heat island of the North-Central Texas region and its relation to the 2011 severe Texas drought. Journal of Applied Meteorology and Climatology. 52: 2418- 2433.

Yannarell, A.C., A.D. Kent, G.H. Lauster, T.K. Kratz, and E.W. Triplett, 2003. Temporal patterns in bacterial communities in three temperate lakes of different trophic status. Microbial Ecology. 46 (4): 391-405.

Biographical Information

Rebekah Ball earned an associate of arts from Tarrant County College followed by a Bachelor of Science in environmental geology and a Master of Science in environmental and earth science at the University of Texas at Arlington. At present she is working as a hydrological technician for the USGS. Her future plans are to become a hydrologist and continue working with the USGS.